UNIVERSITY OF CALIFORNIA SAN DIEGO

The effects of the proteasome inhibitor, bortezomib, on the profile of gene expression in the flatworm pathogen, *Schistosoma mansoni*

A thesis submitted in the satisfaction of the requirements for the Master's of Science

in

Biology

by

Ali A. Syed

Committee in Charge:

Professor Conor R. Caffrey, Chair
Professor Matthew Daugherty, Co-Chair
Professor Jon Christopher Armour

2021

The Thesis of Ali A. Syed is approved, and it is acceptable in quality and form for publication on microfilm and electronically.

University of California San Diego

2021

Dedication

I dedicate this thesis to my amazing family. Without the moral support of my mother, father, and brother I would not have been able to pursue my love of science and accomplish my goals.

Epigraph

“A smooth sea never made a skilled sailor.”

-Franklin Delano Roosevelt

Table of Contents

List of Abbreviations

NTD……Neglected Tropical Disease

DMSO…….Dimethyl Sulfoxide

PZQ…….Praziquantel

BTZ…….Bortezomib

qPCR……Quantitative Polymerase Chain Reaction

RNA-Seq…….Ribonucleic Acid Sequencing

WHO……...World Health Organization

GEP……Gene Expression Profiling

List of Figures

List of Supplemental Figures

List of Tables

List of Supplemental Tables

Acknowledgements

I would like to acknowledge my supervisor, Dr. Conor Caffrey, for helping me to develop my skills as a scientist. The work ethic and attention to detail he has instilled in me will help me throughout my future career as a physician. His support and guidance has also allowed me to nurture and grow my passion for research. Working in his lab has taught me how to apply the basic biological principles that I learned during my undergraduate studies in the laboratory research environment.

I am very grateful to Dr. Nelly El-Sakkary, my post-doctoral mentor, for her guidance and who helped me develop as the scientist I am today. Her dedication to helping, teaching, explaining, correcting and mentoring are greatly appreciated, and I will take everything I have learned from her about science forward into my career, most importantly, how to be a spectacular mentor (teaching someone from square one and to never give up on them).

I'd like to also thank the collaborative members I encountered in the Caffrey team, especially Lawrence Liu and Tony Liu for being amazing friends and helping me whenever I needed it; also, James Pai for starting the project with me, and Supacha Denprasertsuk, Avan Shirwani and Rafay Syed for helping with my work. I thank Zhenze Jiang for being someone to learn from, and, last but not least, Steven Wang for introducing me to the master's program and giving me advice on how to approach it.

It has been the pleasure of my lifetime to work with all of the above people.

Abstract of the Thesis

The effects of the proteasome inhibitor, bortezomib, on the profile of gene expression in the flatworm pathogen, *Schistosoma mansoni*

By

Ali A. Syed

Master of Science in Biology

University of California San Diego, 2021

Professor Conor R. Caffrey, Chair
Professor Matthew Daugherty, Co-Chair

Schistosomiasis is a neglected tropical disease (NTD) caused by flatworm parasites belonging to the genus *Schistosoma.* The disease infects over 200 million people in developing countries where access to clean water is limited. Treatment of schistosomiasis relies on just one drug, praziquantel (PZQ). This drug is only partially effective and resistance is a concern. Together, these encourage the search for new drugs and new drug targets. The proteasome is an essential proteolytic enzyme complex in the cell being responsible for protein turnover. It is a

validated drug target for treatment of certain cancers and a promising target for a number of parasitic infections, including *Schistosoma*. My lab has been using RNA-sequencing (RNA-Seq) to profile the transcriptomic changes after exposure of *Schistosoma mansoni* to the proteasome inhibitor, bortezomib (BTZ). As part of the aims of my project, I provide an initial characterization of the top 300 gene transcripts that were upregulated after treatment of *S. mansoni* with 1 μM BTZ after 12 and/or 24 h *in vitro*. Among these, I identify and discuss heat shock proteins and proteasome subunits that were upregulated at both time points, as well as proteins particular to each time point. Next, using primers that I helped design and then test for efficiency for nine selected genes of interest, I validated the RNA-Seq data via quantitative reverse polymerase chain reaction (qPCR). Lastly, I utilized the Basic Local Alignment Search Tool (BLAST) at the National Center for Biotechnology Information's (NCBI) website to understand whether particular genes of interest are expressed in other developmental stages of the parasite. The resulting data and analysis offer an initial insight into the transcriptomic response of the *S. mansoni* after exposure to a proteasome inhibitor with the goal of identifying new drug targets.

1. Introduction

1.1 Life-cycle

Schistosomiasis or bilharzia is an infectious disease of poverty principally caused by three species of trematode blood flukes, namely, *Schistosoma mansoni*, *Schistosoma japonicum* and *Schistosoma haematobium* (**1-7**). Although the pathologies associated with the different species, including the organs affected, vary, the basic biology regarding the parasite's life cycle including its developmental stages, and the requirement for both a definitive mammalian host and an intermediate molluscan host, is conserved (**Figure 1**).

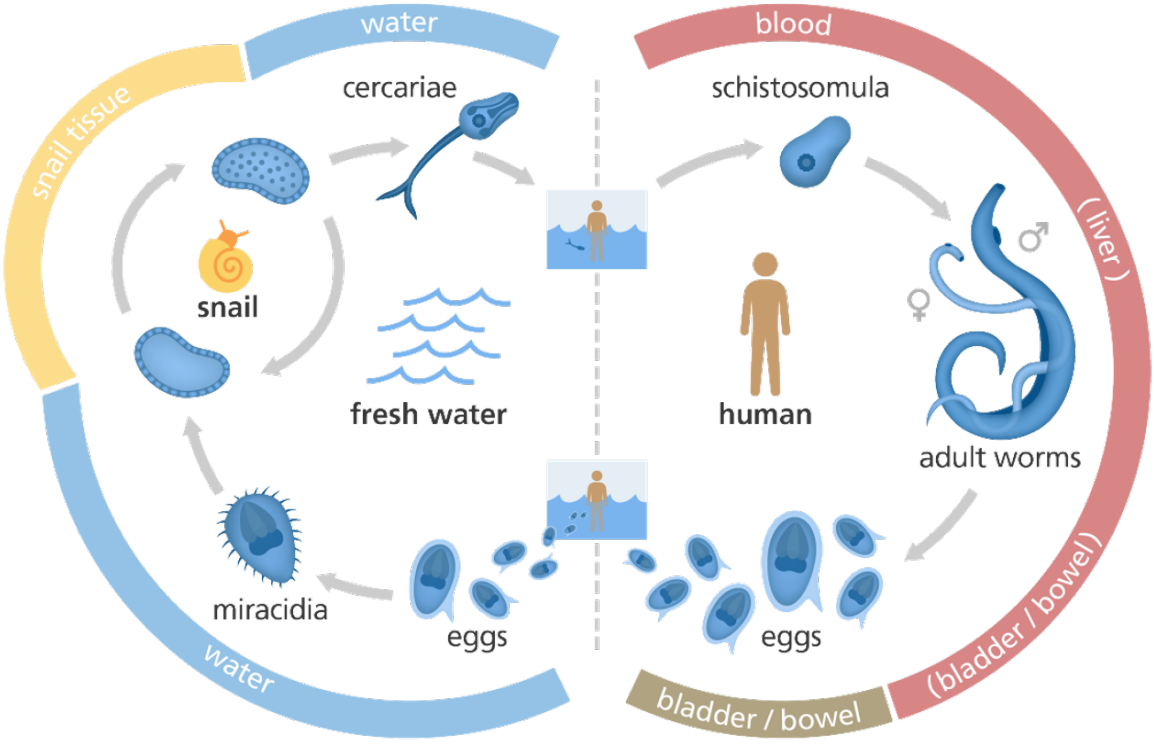

Figure 1. The life cycle of the *Schistosoma* parasite. Each developmental stage is well adapted to survival in either the snail and or mammalian host (**8-10**). Image modified from (**11**).

Using the example of *S. mansoni*, which is the 'model' schistosome most often studied in the laboratory (**12**), adult male and female worms (~ 1 mm in length) reside in the hepatic portal and mesenteric veins of the human host and lay 200-300 eggs/day (**13**). Approximately half of the eggs extravasate, cross the gut wall and are evacuated with the feces (**13**).

The eggs that do escape the body hatch in freshwater (*e.g.*, ditches, canals, streams, and rice paddies) to release a free-swimming miracidium which then seeks out and penetrates the molluscan intermediate host (*Biomphalaria* spp. in the case of *S. mansoni*). Once established in the snail, the parasite (comprising sporocysts) asexually reproduces for approximately 4-6 weeks and egresses as thousands of free-swimming cercariae which then seek out the mammalian host. Cercariae penetrate the skin, and after two weeks of migration through the heart and lungs, establish themselves in the hepatic portal and mesenteric nervous system. After a further two-week period of maturation followed by mating, male and female worms commence egg production (**8**).

Unique among platyhelminth flatworms, the schistosome is dioecious (**14-16**). Each male supports one female in a specialized gynaecophoric groove that runs down the male's long axis. Males essentially chauffeur the thinner and less muscular females around the mesenteric system as she lays her eggs (each ~150 x 70 μm). Females rely on this close contact with males to maintain maturation and egg-laying, otherwise, they revert to an immature non-reproductive state (**17,18**). A single adult worm's lifespan is believed to be about a decade; however, cases of active human schistosomiasis (*i.e.*, fresh eggs being found in body wastes) have been identified many decades after infection (**19,20**).

1.2 Immunopathology, clinical signs, and comorbidities

The approximately 50% of eggs that do not escape the body become trapped in the viscera, notably the liver and bladder for *S. mansoni* and *S. haematobium*, respectively, where they elicit an inflammatory immune response that ultimately induces fibrosis of the affected tissues (**21**). Both *S. mansoni* and S. *haematobium* eggs elicit interleukin-1 agonist (IL-1a), IL-10 and tumor necrosis factor-α (TNFα), which trigger inflammation (**22**). The inexorable fibrotic degradation of organ performance over decades of infection can lead to severe and, eventually, life-threatening liver fibrosis, renal failure, chronic hematemesis, hematochezia, ureteric obstruction resulting in hydronephrosis and various cancer pathologies (**1,22-25**). In some chronic cases, cerebral symptoms such as delirium, cerebral hernia, seizures, visual disturbances and intercranial hypertension, as well damage to the spine that can lead to sensory loss, have occurred (**26**). In children, growth retardation, malnutrition and poor cognitive function have all been recorded as a consequence of schistosome infection (**21**). In women, female genital schistosomiasis (FGS) adversely impacts fertility and childbirth (**25**). The increased risk of acquiring sexually transmitted diseases, not least HIV, due to FGS is a growing concern for the World Health Organization (WHO) (**27**).

Apart from these severe consequences of infection for the individual, the most common symptoms associated with schistosome infection include pain and malaise that limit the ability to perform manual labor, which, in turn, contribute to maintaining economic poverty in subsistence communities.

1.3 Prevalence, distribution and treatment

Currently, the WHO reports that schistosomiasis infects almost 240 million people worldwide with more than 700 million people are at risk (**28**). The disease is found in 52 developing countries in sub-Saharan Africa, South-east Asia and South America, notably Brazil (**Figure 2**). Those most at risk live have limited or no access to clean water and proper sanitation, and instead rely on natural water sources such as freshwater streams and rivers for everyday activities, from cooking to washing to removing body wastes (**5**).

Treatment and management of schistosomiasis rely on just one drug, the amino-quinolone, praziquantel (PZQ). Developed as an animal health drug by Bayer and Merck in the early 1970s, PZQ is active against all schistosome species but at the recommended single oral dose of 40-60 mg/kg offered to humans, its efficacy is highly variable, ranging from 50-90% cure (**29**). This deficiency complicates national and regional strategies to eliminate and eventually eradicate the disease. Administering more than one dose increases efficacy, however, this is logistically challenging to manage in the vertical drug delivery programs that many developing countries rely on for worm control in general (**29-32**).

Apart from its modest efficacy, there are concerns regarding drug resistance, especially as delivery programs expand to treat more people more often (**33,34,35**). Evidence of resistance has been detected in Egypt and Senegal (**36**). Also, resistance has been demonstrated in mouse models of *S. mansoni* infection (**37**). Possible mechanisms underlying resistance include increased expression of ATP-binding cassettes or changes in the parasite's calcium channels. (**5**,**6**,**29,37,38**).

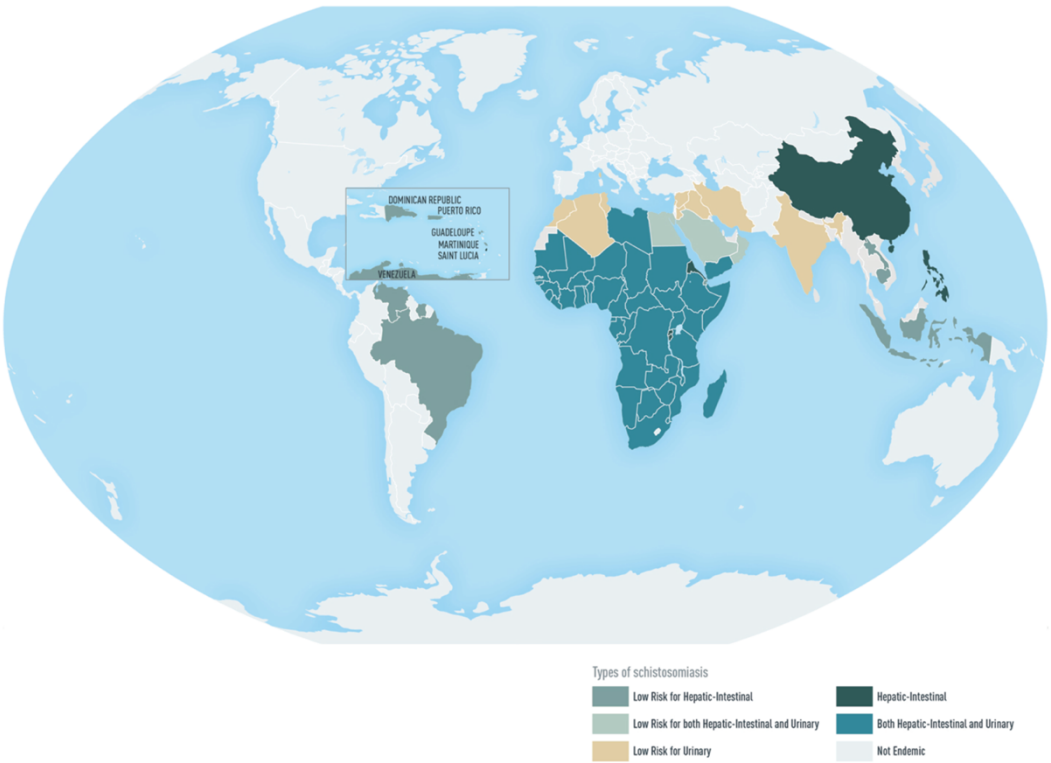

Figure 2. Distribution of schistosomiasis. Taken from (**30**).

1.4 The 20S proteasome as a potential drug target for the treatment of schistosomiasis

With the reliance on a single drug for treatment and control of schistosomiasis and the pharmaceutical industry's lack of investment in what is a disease of poverty, academia has a significant contribution to make in the identification of new drugs and drug targets (**39-44**). Research over the last ten years has shown that the 20S proteasome is a viable target for the treatment of other parasitic diseases, including those caused by the plasmodial (malaria) parasite and *Leishmania* (**39,45-48**). Recent research by my PI, Conor Caffrey, in collaboration with his faculty colleague, Anthony O'Donoghue at the Skaggs School of Pharmacy and Pharmaceutical Science, has highlighted the importance of the 20S proteasome to the survival of *S. mansoni* (**49,50**), as described below.

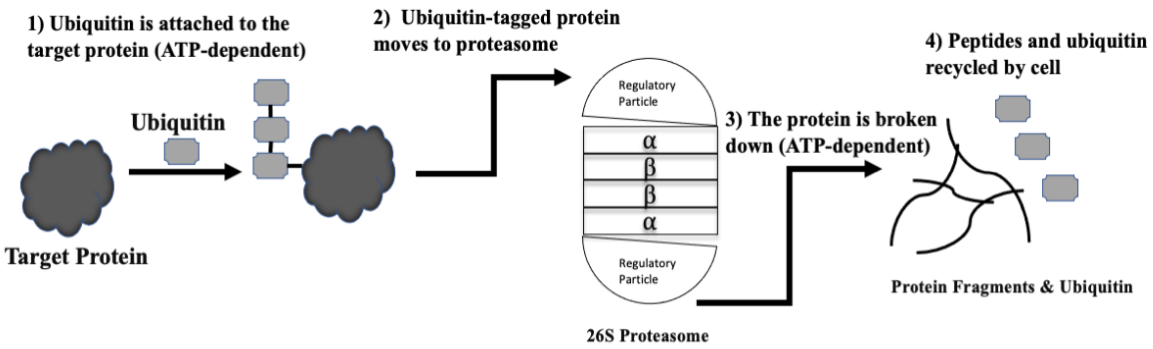

Figure 3. The basic process by which a protein is marked for degradation by the proteasome.

The multi-catalytic proteasome complex is central to maintaining normal protein turnover in eukaryotes and is required for survival (**42**). Damaged or misfolded proteins are tagged with ubiquitin that then targets the proteins for proteasomal degradation and reutilization of the component peptides and amino acids by the cell (**42**) (**Figure 3**). The 26S proteasome is composed of two main sub-complexes, the 20S barrel-shaped catalytic core and the 19S regulatory subunits that cap both ends (**42**). The apical 19S regulatory subunit has several functions, including recognizing, binding and unfolding ubiquitin-tagged proteins and gating their entry into the catalytic core. The 20S catalytic core comprises four rings, each with seven α and β-subunits. The α-subunits are catalytically inactive, whereas the β1, β2 and β5 catalytic subunits cleave proteins with activities described as caspase-, trypsin- and chymotrypsin-like, respectively (**49**). One or more of these β subunits is the principal target of current proteasome inhibitor drugs, as described below.

1.5 Small-molecule inhibitors of the 20S proteasome kill *S. mansoni*

Proteasome inhibitors as drugs first found clinical application in the treatment of multiple myeloma (**51-54**). Bortezomib (BTZ; Velcade® by Takeda; **Figure 4**) covalently binds to the

active site threonine in the β5 subunit and less so with the β1 active site (**55**). Carfilzomib (CFZ; KYPROLIS® by Amgen; **Figure 4**) binds specifically to the β5 subunit N-terminal threonine (**55**). Key differences between the two proteasome inhibitors is that the boronic acid reactive group of BTZ binds reversibly and the molecule has some off-target binding, whereas the epoxide of CFZ binds irreversibly and the molecule has minimal off-target binding (**56,57**). BTZ's off-target binding has been associated with side effects during the treatment of multiple myeloma and other cancers (**57**,**51**).

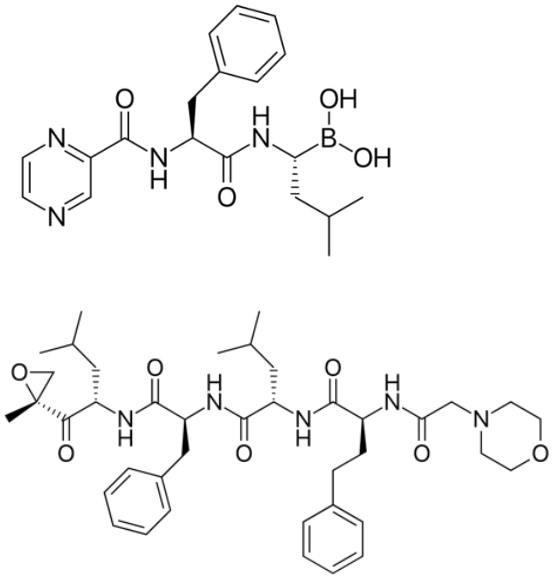

Figure 4. Structures of BTZ and CFZ. BTZ (top) possesses a boronic acid reactive group whereas CFZ (bottom) has an epoxide group.

In the last 15 years, proteasome inhibitors have been investigated as a possible treatment for parasitic infections (**39,48**). Research with *Leishmania donovani* has shown that proteasome inhibition stops cell division, possibly due to blockade of the G2/M checkpoint in cell cycling (**45,48**). For *Plasmodium falciparum,* inhibition of the β5 subunit, with co-inhibition of either the β1 or β2 subunits, results in the selective anti-malarial compounds with decreased toxicity to the

mammalian host (**58**). For *S. mansoni*, recent work has demonstrated that both BTZ and CFZ interfere with the motility and viability of the parasite *in vitro*, and that these effects are associated with inhibition of the Sm20S schistosome proteasome target. Inhibition of Sm20S induces apoptosis which, in mammalian cells, is typically associated with disruption of proteasome function (**49**) (**Figure 5**).

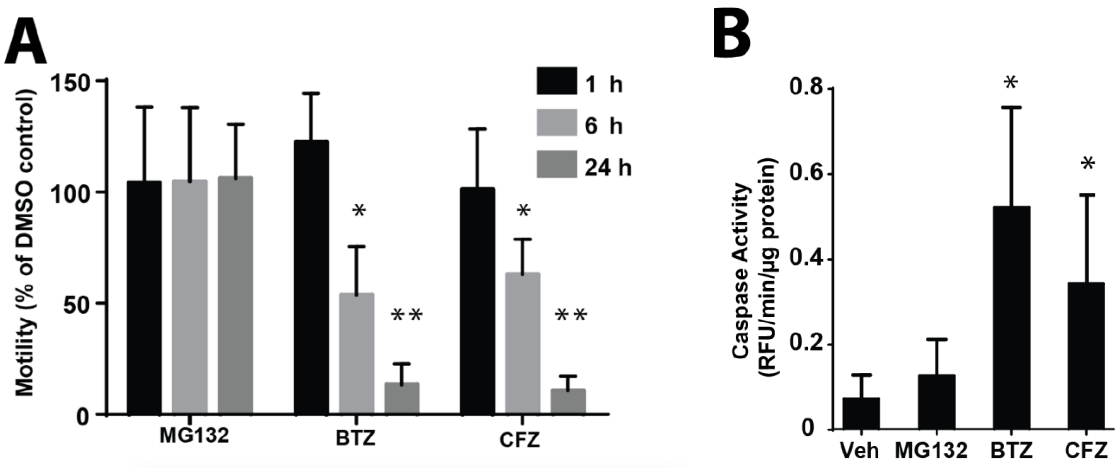

Figure 5. BTZ and CFZ decrease adult *S. mansoni* motility and induce caspase activity. A. Decreased worm motility as a function of time for three proteasome inhibitors. **B.** Induction of caspase activity after a 24 h incubation with proteasome inhibitors. Both **A** and **B** are taken from (**49**). MG132 is peptide aldehyde inhibitor of the proteasome (**49**).

As part of my lab's research program, RNA-sequencing (RNA-Seq) is being used to understand the global transcriptomic changes in biological pathways and proteins after incubation of adult *S. mansoni* with proteasome inhibitors. Understanding these changes could help identify new drug targets for disease intervention, as has been shown in many other biomedical contexts (**59,60**).

2. Aims of this thesis

The methods described here regarding RNA-Seq and the assembling of the data sets arising were primarily performed by my post-doctoral supervisor, Dr. Nelly El-Sakkary (*El-Sakkary et al.,*

2021, in preparation). These descriptions are contextually relevant for the aims of my thesis which are to (i) initially characterize the top 300 gene transcripts upregulated after treatment of *S. mansoni* with 1 μM BTZ after 12 and 24 h *in vitro,* (ii) for nine chosen genes, validate the RNA-Seq data using the quantitative reverse polymerase chain reaction (qPCR), and (iii) understand whether the particular genes of interest are expressed in other developmental stages of the parasite via BLAST analysis of the available expressed sequence tag (EST) information. For these three aims, I discuss my findings in relation to the literature.

3. Materials and Methods

3.1 Purchase and maintenance of proteasome inhibitor stocks.

BTZ (Selleckchem, TX, USA) and CFZ (UBPBio, TX, USA) were diluted to 10 μM in DMSO and frozen at -80℃ as 1 mL aliquots until use.

3.2 Harvesting *Schistosoma mansoni* adults

Male Golden Syrian hamsters were infected percutaneously at four weeks of age with 600-800 *S. mansoni* cercariae. Seven weeks after infection, hamsters were euthanized with an overdose of sodium pentobarbital solution (Fatal-Plus; Vortech Pharmaceuticals Ltd, MI, USA). Adult worms were then harvested by reverse perfusion of the hepatic portal system (**40,41**,**61,62**). The maintenance and handling of hamsters were carried out in accordance with a protocol approved by the Institutional Animal Care and Use Committee (IACUC) of the University of California San Diego.

3.3 Exposing *S. mansoni* to BTZ *in vitro*

After extensive washing, adult *S. mansoni* worms were cultured in 24 well plates (# 3544, Corning Inc, NY, USA) at five males/well in 1 mL Basch medium (**41**) containing 4% heat-inactivated FBS, 100 U/mL penicillin and 100 µg/mL streptomycin. Worms were acclimated overnight at 37ºC in a 5% CO_2 atmosphere. Next morning, BTZ in DMSO was added and the same medium added to a final volume of 2 mL (final BTZ concentration was 1 µM). Parasites were incubated at 37ºC and 5% CO_2 for 12 or 24 h. Negative controls comprised worms incubated with DMSO vehicle at a final concentration of 0.5%.

3.4 RNA Extraction

Two wells in the 24 well plate, comprising 10 worms, were combined to extract one RNA sample with three RNA samples per perfusion. One perfusion was used to derive RNA after incubation for 12 h with BTZ whereas three perfusions were used for the 24 h time point. For each RNA extraction, worms were pooled into 1.5 mL tubes (Thermo Fisher Scientific, MA, USA), washed four times with PBS, resuspended in 50 µL TRIzol (Thermo Fisher Scientific, Inc., MA, USA) and snap frozen over dry ice for storage at – 80ºC. Worms were homogenized with a pestle in 800 µL TRIzol and the homogenate was transferred to a 2 mL tube filled with zirconia-silica beads (#S6012-50, Zymo Research, CA, USA). The homogenate was vortexed in a Fisher Scientific Analog Vortex Mixer (Cat #02215365, Model # 945404, Waltham, MA, USA) at the maximum setting (50,160 Hz = 1 phase) for 6 min, placed on ice for 2 min, and the step repeated again. Once vortexed, 100% ethanol was added and the homogenate applied to the Zymo kit-

provided column, according to the manufacturer's instructions (Direct-zol RNA Miniprep, #R2051, Zymo Research, CA, USA) to complete the extraction of the RNA.

The concentration of RNA was determined using a Nanodrop (ND2000, Thermo Fisher Scientific, Inc., MA, USA). This machine measures absorbance at 260 nm to calculate the RNA concentration (minimum 50 ng/µl acceptable) and the 260 nm:280 nm (RNA:protein) ratio (minimum of 1.8 acceptable) for an initial assessment of sample purity. A subsequent quality assessment is performed by the UC San Diego Institute for Genomic Medicine (IGM) services center using the electropherogram-based Agilent 2100 Bioanalyzer (Agilent Technologies, CA, USA). This machine employs microfluidics to separate fluorescently-bound RNA in microchannels based on size to generate an electropherogram, which is a graphical output resembling a gel image that indicates fluorescent units (FU). Ribosomal (r)RNA is used as an indicator of RNA quality. Because schistosomes lack the 28S rRNA that is typically compared with 18S rRNA to derive the RNA Integrity Number (RIN), which is a measure of RNA quality (**54**), we used the intensity of the 18S peak (>4000 FU) compared to the intensity of other RNA in the sample (<1000 RFU) to evaluate RNA quality.

3.5 cDNA library construction and RNA-sequencing (RNA-Seq)

cDNA library constructs and adaptor-ligated gene fragments were synthesized using a TruSeq Stranded Total RNA Ribo-Zero H/M/R Gold kit (Illumina Inc., CA, USA) at the IGM using 100 ng of RNA per library. Each library was sequenced in an Illumina HiSeq 4000 sequencer by single-end reads of 75 base pairs (SR75). For the 12 h time point, three cDNA libraries (one library per RNA sample) from the single perfusion were sequenced, whereas for the 24 h time point, five cDNA library samples were sequenced from three separate perfusions.

Data from a sequencing run were visualized in an MA plot (an application of the Bland–Altman plot which is the same as the Tukey mean-difference plot) (**64**) that was generated using the ROSALIND™ software (OnRamp Biotechnologies Inc., San Diego, CA) (**65**). The plot visualizes the differences between two sequencing runs by transforming the data onto M (log ratio) and A (mean average) scales and then plotting those values. Although each of the two sequencing runs performed for each time point had different absolute expression values (attributable to variations in the sensitivity of RNA-Seq due to slight environmental and handling differences), the overall fold change values showed the same patterns of increases in expression. Ultimately, we analyzed one sequencing run for each of the time points as described below.

3.6 RNA-Seq analysis

RNA-Seq data were generated in the FASTq format with each file being approximately ~500 MB in size. The files were analyzed using the ROSALIND™ software (OnRamp Biotechnologies Inc.) (**65**) which uses HyperScale architecture, a tool developed by OnRamp, to map reads. Each library was normalized by determining the Relative Log Expression (RLE) using Differential gene Expression analysis that is based on the negative binomial distribution (DESeq2) (**66**). DESeq2, which is available as a package in R (RStudio, Boston, MA), was used to calculate both the relative gene expression (as fold changes) compared to DMSO controls and the associated p-Adjusted (P-Adj) values ($\leq$ 0.05 significance cutoff). DESeq2 uses covariate correction and negative binomial generalized linear models to estimate the dispersion and logarithmic fold changes, and incorporate data-driven prior distributions. It also automatically identifies outlier genes using Cook's distance and then removes them from the analysis (**67**).

Following the determination of fold-expression changes and P-Adj values by DESeq2, the Partitioning Around Medoids (PAM) algorithm was used in ROSALIND™ to partition the RNA-Seq data into heat-maps. In addition, enrichment analysis of pathways, gene ontology and domain structure analyses were performed in ROSALIND using the tool, "Hypergeometric Optimization of Motif EnRichment (HOMER)" (**68**). HOMER is available online (http://homer.ucsd.edu/homer/) and allows the quantification of RNA-Seq transcripts for gene expression analysis.

3.7 cDNA Synthesis prior to qPCR

Worms were exposed to proteasome inhibitor or DMSO, as described in Section 3.3. Total RNA was extracted using a kit (#R2051, Zymo Research® , CA, USA) and cDNA synthesized from 1 µg RNA using the SuperScript™ VILO cDNA Synthesis Kit (#11754050, Thermo Fisher Scientific Inc., MA, USA) according to the protocol supplied. The resulting cDNA concentration was determined via Nanodrop. Wavelength ratios at 260 nm:230 nm and 260 nm:280 nm were measured, and the respective values of 1.60-1.90 and 1.90-2.05 indicated the minimal contamination by carbohydrate, or phenol and protein, respectively (**69**). Samples were frozen at –80°C until use.

3.8 Designing primers for qPCR validation of selected upregulated gene transcripts

After incubation of *S. mansoni* with 1µM BTZ for 12 and/or 24 h, (**Suppl. Table 1**), 34 gene transcripts were initially selected for qPCR analysis. Forward and reverse primers were designed for each target using the NCBI primer design tool (**70**). Primers had no more than 12 consecutive nucleotides that paired with other genes in the *S. mansoni* genome to minimize off-target (non-

specific) binding. Primers were also selected based on a GC content >55%. Using these criteria, qPCR primers for 11 genes (including two control gene transcripts unaffected by proteasome treatment) were eventually selected and ordered from Thermo Fisher Scientific (**71**) (**Table 1**).

Table 1. Gene targets for qPCR validation and their final primer efficiencies

Gene ID[a]	Category	Gene Description	Fold Change	P-Adj Value	Primer Efficiency
Smp_049250	Stress Response	Heat shock protein-HSP20/α-crystallin family	11.48	7.74E-11	107%
Smp_106930	Stress Response	Heat shock 70 kDa protein homolog	13.19	2.73E-15	92%
Smp_123260	Apoptosis/Proteasome Pathway Genes	Ubiquitin 1	5.08	1.29E-06	114%
Smp_171150	Cell Regulation	Shk1 kinase-binding protein	2.33	0.040085	112%
Smp_102240	Cell Regulation	Upf3 regulator of nonsense transcripts-like protein	2.06	0.000116	107%
Smp_072340	Proteasome	26s proteasome regulatory subunit 6b	1.94	0.001843	105%
Smp_052870	Proteasome	26s proteasome non-ATPase regulatory	1.55	4.03E-15	112%
Smp_119310	Proteasome	26s protease regulatory subunit	1.59	0.00417	103%
Smp_067890	Proteasome	Proteasome subunit α-type	1.54	0.03138	107%
Smp_165020	*Control*	*Transmembrane 9 superfamily protein member*	*1.00*	*N/A*	112%
Smp_044920	*Control*	*Dynamin*	*1.00*	*N/A*	114%

[a]Nine target and two control gene transcripts for amplification by qPCR. By RNA-Seq, the nine target transcripts were determined to be significantly upregulated with a fold change ≥ 1.5 and a P-Adj value ≤ 0.05.

3.9 Measuring primer efficacy and performing qPCR

Primer efficiency ensures that cDNA amplification with a specific primer set under a set of qPCR conditions is as close to 100% as possible such that the data arising are a true reflection of mRNA

abundance (**72**). Primer efficiency was evaluated over an eight-fold dilution series in water containing 5 to 1,000 ng total cDNA from worms that had been incubated in the presence of 0.5% DMSO for 24 h. Control qPCR reactions without cDNA were also prepared. Reactions were set up in the Thermo Fisher Scientific 12-tube strip (#AB1112) and cap (#AB0783) system. qPCR samples each contained 10 µL PowerUp™ SYBR Green Master Mix (Thermo Fisher Scientific #A25741), 1.3 µL of each of the forward and reverse primers (10 µM final), 1 µL cDNA at the tested concentration and 6.4 µL water for a total of 20 µL. Using the Thermo Fisher Scientific primer efficiency calculator, efficiency was considered acceptable when it fell in the range of 85-115% which is consistent with the current literature on qPCR primer efficiencies (**73-76**). To achieve optimal efficiency, the cDNA concentration and primer melting temperature (T_m) were adjusted. Efficiencies were calculated using the equation $10^{[(-1/slope)-1]} * 100\%$ and plotted.

Once optimal primer efficiency had been achieved, qPCR was performed in a Mx3005p thermocycler (Agilent Technologies, CA, USA). Samples contained 10 µL SYBR Green Master Mix, 1.4 µL forward and reverse primers (10 µM final), 1 µL (1 µg) cDNA and 6.2 µL water. Conditions for cycling were 50°C/2 min, 95°C/2 min, and followed by 46 cycles of 95°C/15 sec (denaturing), 58°C/15 sec (annealing) and 72°C/1 min (extension). Smp_165020 (transmembrane 9 superfamily protein member) and Smp_044920 (dynamin) were used as control genes (**Table 1**). cDNA was synthesized from the RNA of worms (from two separate perfusions) that had been exposed to 1 µM BTZ or DMSO for 24 h. qPCR was performed on each sample in triplicate, *i.e.*, six replicates total. The qPCR data from the six replicates were averaged and two-sided (two-tailed) *t*-tests were performed in MS Excel to determine p-values relative to DMSO controls. Also, the standard error of the means (SEMs) was calculated across the six replicates to measure the variability between qPCR runs.

Relative gene expression was calculated using the delta-delta Ct method (**77**). This method takes the threshold amount of amplification, measured as relative fluorescence units (RFU), in our case 3,000 RFU, and compares the number of PCR cycles needed to reach the RFU threshold. Upregulated genes will need a relatively fewer number of cycles of PCR to achieve the threshold compared to control genes.

3.10 Manual characterization of transcripts and stage-specificity of expression

Based on the current annotation of the *S. mansoni* genome (**50**), 516 (40%) of the 1,350 gene transcripts that had been upregulated as consequence of BTZ exposure for 24 h were annotated as 'unknown' or 'uncharacterized.' For BTZ at 12 h, 248 of 615 (40%) upregulated genes were uncharacterized. For the top 300 upregulated transcripts, we attempted to manually characterize these unknowns using the NCBI's nucleotide (BLASTn) and protein (BLASTp) BLAST algorithms (https://blast.ncbi.nlm.nih.gov/Blast.cgi) (**78,79**). Specifically, on the NCBI's splash page, the Smp gene identifier was entered and the search executed. Under the 'gene' information returned, the associated mRNA "XM" identifier was clicked to locate the gene's complete mRNA sequence. The BLASTn algorithm was executed on this sequence by constraining the search to the Expressed Sequence Tags (EST) database and organism ID, namely *Schistosoma mansoni* (code 6183). The list of returned hits was scrolled through line by line using the following minimal criteria for acceptance of a hit: max score >300; query coverage >20%; percent identity >75%. Sequences associated with the egg (identified as ME), sporocyst (MG), miracidium (ML), schistosomulum (MS), cercaria (MC), and adult males (MA) and females (MF) were noted and the information used to populate **Table 2.**

For those transcripts that had been manually characterized, we then interrogated their putative function(s) using the Kyoto Encyclopedia of Genes and Genomes (KEGG) pathways database (https://www.genome.jp/kegg/) (**80**).

4. Results

4.1 Gene expression profiling (GEP) of *S. mansoni* adults after exposure to BTZ

We performed GEP of the RNA-Seq data from adult, male *S. mansoni* that had been exposed *in vitro* to 1 μM BTZ for 12 and 24 h. The top 300 upregulated genes for BTZ at 12 and 24 h were grouped based on a KEGG category analysis.

Comparing the 12 and 24 h time points for BTZ-exposure, 95/300 (~32%) were commonly upregulated *vs*. DMSO control, (intersection of the Venn diagram in **Figure 6**) whereas 205 genes were uniquely upregulated at each time point (exclusive areas of the Venn diagram). Based on the annotation of the *S. mansoni* genome, 40, 76 and 49 of the genes common to both time points, and the 12 and 24 h time points, respectively, had been uncharacterized. After manual characterization, 16, 26 and 37 genes remained uncharacterized, respectively. The complete list of the 95 common and 205 exclusive gene transcripts, and their fold changes in expression and p-Adj values is shown in **Supplemental Table 1**.

The KEGG categories identified among the 95 common characterized sequences included the large category, *genetic information and processing*, and its subcategories, *transcription*, *translation* and *heat shock proteins*. The common gene transcripts included various stress response heat shock protein (HSP) genes such as Smp_049250 (SmHSP20; 8.93- and 11.48-fold upregulated at 12 h and 24 h, respectively), Smp_049240 (SmHSP27; 7.05- and 4.24-fold upregulated at 12 h and 24 h, respectively), Smp_106930 (SmHSP70; 12.96- and 13.18-fold upregulated at 12 h and 24 h, respectively) and Smp_072330 (SmHSP86; 6.60- and 4.28-fold upregulated at 12 h and 24 h, respectively). Also included were proteasome subunit genes, such as Smp_042270 (26S protease regulatory subunit 6a; 2.36- and 1.69-fold upregulated at 12 h and 24 h, respectively), Smp_067890 (proteasome subunit-α; 1.88- and 1.54-fold at 12 h and 24 h,

respectively), and Smp_121430 (proteasome subunit-β, 1.87- and 1.53-fold upregulated at 12 h and 24 h, respectively).

Among the upregulated gene transcripts that were particular to the 12 h timepoint were Smp_085740, (abl-interactor (Abi) protein; 1.7-fold upregulated), Smp_011600 (connector enhancer of kinase suppressor of ras 2 (CNKSR2); 2.2-fold upregulated) and Smp_140630 (TELO2-interacting protein 1 (Tti); 1.9-fold upregulated). Likewise, for the 24 h timepoint, upregulated transcripts included Smp_210400 (ATP-dependent Clp protease proteolytic subunit; 1.6-fold upregulated), Smp_011960 (Inositol-pentakisphosphate 2-kinase; 2.6-fold upregulated) and Smp_172200 (tyrosine kinase; 2.4-fold upregulated).

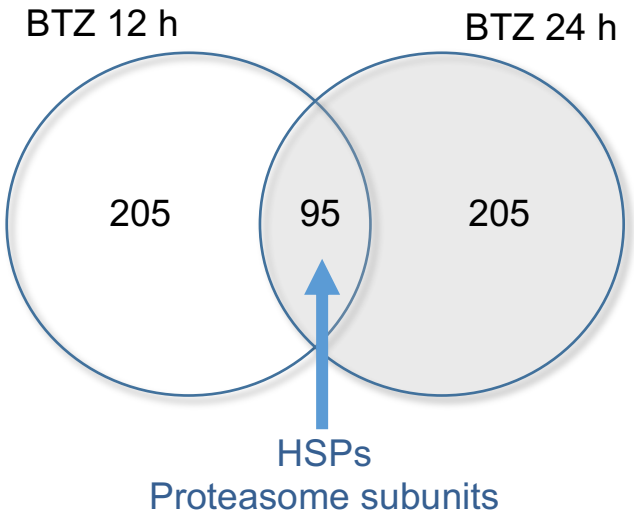

Figure 6. Venn diagram of common and exclusively upregulated genes following exposure of *S. mansoni* to BTZ. Among the top 300 most upregulated gene transcripts for BTZ at 12 and 24 h, 95 transcripts were common to both time points whereas 205 transcripts were exclusively to either time point. All transcripts were significantly upregulated with a fold change ≥ 1.5 and a P-Adj value ≤ 0.05. HSP = heat shock protein. The Venn diagram was generated as described in the Suppl. Methods.

4.2 Primer efficiency and validation of RNA-Seq data

An initial set of 34 transcript targets which had been upregulated after exposure to BTZ for 24 h was chosen for qPCR primer design and RNA-Seq validation. These primers were whittled down to a final set of nine, plus two controls, based on the selection criteria outlined in **Section 3.8**. Once selected, each pair required three to five qPCR test runs to establish optimal efficiency: the final efficiencies are reported in **Table 1** and all 11 final efficiency curves are presented in **Supplemental Figure 1**.

Once primer pair efficiency had been optimized, qPCR was performed. The data generated for the fold-change in the upregulation of genes of interest agree to a statistically significant degree with those measured by RNA-Seq (**Figure 7**) suggesting that the RNA seq data, as a whole, are accurate.

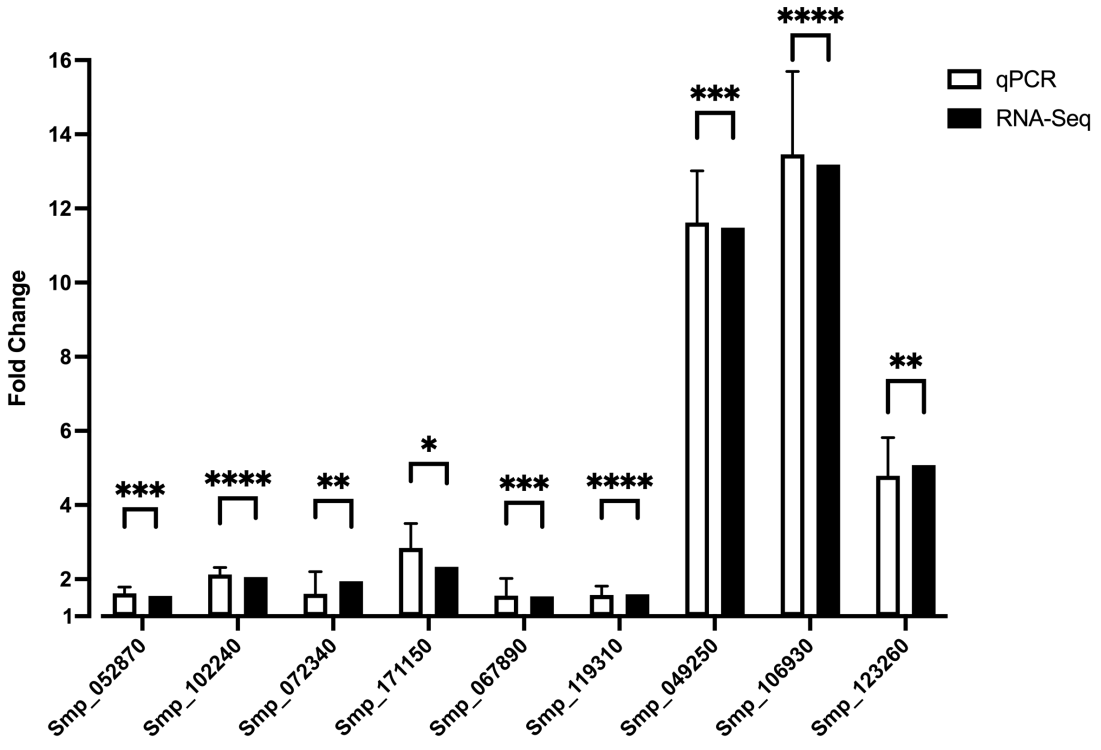

Figure 7. qPCR validation of RNA-Seq data after a 24 h exposure to 1 µM BTZ. qPCR data were analyzed using the $\Delta\Delta C_T$ method. Smp_165020 and Smp_044920 were used as control genes. Student's two-sided *t*-test p-values (*p<0.05, ** p<0.005, *** p<0.0005, **** p<0.00005) were calculated to show significance with respect to the RNA-Seq data.

4.3 Stage-specific expression of genes exposed to BTZ for 24 h

For the top 20 genes upregulated after exposure to BTZ for 24 h, including the nine target genes validated by in qPCR, we used the NCBI BLASTn and BLASTp tools to query the *S. mansoni* EST data and understand whether the genes of interest were expressed in other developmental stages of the parasite. As shown in **Table 2**, those genes with the greatest distribution across the various stages include the HSPs, Smp_106930, Smp_049250, Smp_049240 and Smp_072330, and the proteasome subunit/regulatory genes Smp_119310, Smp_102240, Smp_052870 and Smp_072340. Some genes could not be identified in the different stages due to either their true absence or the absence of EST data.

Table 2. Expression of the top 20 upregulated in genes and our selected qPCR genes in different developmental stages of *S. mansoni*

Name	Description	Fold Change[a]	P-Adj	ME[b]	MG	ML	MS	MC	MA	MF
Smp_106930*	Heat shock 70 kDa protein homolog	13.19	2.73E-15							
Smp_049250*	Heat shock protein-HSP20/α-crystallin family	11.48	7.74E-11							
Smp_149750	Uncharacterized protein	7.62	3.86E-09							
Smp_048050	α-Crystallin A chain	6.03	1.97E-07							
Smp_049300	Major egg antigen	5.89	2.60E-05							
Smp_049230	Heat shock protein HSP16	5.61	1.97E-07							
Smp_133770	Glutamine synthetase bacteria	5.61	5.51E-06							
Smp_185680^	Major egg antigen	5.58	5.11E-05							
Smp_123260*	Ubiquitin 1	5.08	1.29E-06							
Smp_138080	MEG-3 (Grail) family	4.92	0.000124							
Smp_176110^	Leucine rich repeat-containing domain	4.86	1.29E-06							
Smp_040680	Cytoplasmic dynein light chain	4.72	5.47E-09							
Smp_138070	MEG-3 (Grail) family	4.56	0.000324							

Table 2. (Cont.)

Smp_138060	MEG-3 (Grail) family	4.47	0.000451							
Smp_003600^	Natterin-4	4.41	0.000347							
Smp_072330	Heat shock protein (HSP86)	4.28	9.59E-08							
Smp_049240	Heat-shock protein β-1	4.24	0.000548							
Smp_072460	Phosphomevalonate kinase	4.01	3.26E-05							
Smp_200900	Uncharacterized protein	3.81	4.08E-06							
Smp_067890*	Proteasome subunit α-type	1.54	0.003138							
Smp_119310*	26s protease regulatory subunit	1.59	0.00417							
Smp_102240*	Upf3 regulator of nonsense transcripts-like protein	2.06	0.000116							
Smp_052870*	26s proteasome non-ATPase regulatory subunit	1.55	4.03E-15							
Smp_072340*	26s protease regulatory subunit 6b	1.94	0.001843							
Smp_171150*	Shk1 kinase-binding protein	2.34	0.040085							

[a] For the top 20 genes upregulated after exposure to BTZ for 24 h and our selected qPCR genes.
[b] Terms: ME, egg; MG, germball (sporocyst); ML, miracidium; MS, schistosomulum; MC, cercaria; MA, mixed-sex adult; MF, adult female. Empty cells indicate that no EST sequence data were found.
* indicates the nine qPCR-validated genes.
^ indicates EST data identified using the BLASTp tool, otherwise the BLASTn tool was used.

5. Discussion

Schistosomiasis is a disease that affects more than 240 million people worldwide and over 700 million people are at risk of contracting infection (**28**). Disease-treatment and control rely on just one partially effective drug, praziquantel (**29-32**) and concerns regarding the emergence of resistance to this essential drug spur research into new drugs and drug targets (**36-37**). The research presented here is part of a larger project to investigate the schistosome proteasome as a drug target which follows the validation of the proteasome as a target for the treatment of other parasitic diseases, such as *Plasmodium* and *Leishmania* (**39,45-48**), and the treatment of multiple myeloma (**51,52,57**).

The first aim of my research was an initial understanding of what principal genes are upregulated by adult *S. mansoni* in response to proteasome inhibition by BTZ at both the 12 and 24 h time points. A complete pathway analysis is beyond the scope of this thesis, however, it was clear that a number of genes with related functions were upregulated in response to BTZ. First among these were the HSPs. Six different HSPs (Smp_106930, Smp_049250, Smp_049240, Smp_072330, Smp_069130 and Smp_008545) and one HSP-interacting protein (Smp_064860) were upregulated by between 2.2- and 13.2-fold over both time points compared to the DMSO control (**Supplemental Table 1**). The evolutionarily conserved HSPs (**81**) comprise six families of protein chaperones (**82**) that facilitate protein-folding, -unfolding and -transport (**83**), and are upregulated in response to stress (*e.g.*, heat, oxygen deprivation or, indeed, proteasome inhibition (**84**)) in order to protect the functionality of vital cell proteins during a stress event (**85**).

Smp_106930 and Smp_049250 warrant discussion as they are the most upregulated of all 95 proteins after both 12 h (12.96 and 8.92-fold upregulated, respectively) and 24 h (13.18 and 11.48-fold upregulated, respectively) in the presence of BTZ. Smp_106930 is orthologous to the first HSP discovered, namely HSP70 (**86**), itself part of a family of ~70 kDa proteins that make

vital contributions to the stress response in eukaryotic cells (**87**) and have pro-survival functions in cancer cells (**88**). In *Plasmodium*, HSP70 has key transcription control capabilities under the heat-stress conditions that occur during fever episodes (**89,90**). In *S. mansoni*, Smp_106930 (aka SmHSP70) is an immunogen that generates an antibody response in mice, baboons and humans infected with the parasite (**91**), and has potential as a diagnostic antigen (**92**). SmHSP70 may also aid *S. mansoni* cercaria in locating the mammalian host (**93**).

Smp_049250 encodes an α-crystallin small HSP (SmHSP20) which, like HP70, is a stress responder, in addition to having other functions such as protein transport (**94,95**) and stabilization of the cytoskeleton (**96,97**). In *Plasmodium*, HSP20 acts as a transporter protein for HSP70 as part of the stress-induced induction of transcription (**89,90**). SmHSP20 (**Table 2**), like SmHSP70, is a major immunogen during infection (**98**) and an homolog of p40 which is found in the secretions of cercaria where it may act as a chaperone protein (**99**).

In other eukaryotic systems, both HSP70 and HSP20 are upregulated in response to proteasome blockade (**100-102**) and our findings are consistent with those data. As discussed for these other systems, the upregulation of SmHSP70, SmHSP20, and perhaps the other upregulated SmHSPs identified here, may represent an attempt by the parasite to counteract the cell stress response resulting from proteasome inhibition. As vital survival proteins, it is not surprising that both HSP70 and HSP20, and some of the other HSPs, are expressed across most of the different developmental stages of the schistosome parasite (**Table 2**). In future, the strong upregulation of both the HSP70 and HSP20 genes will be verified at the protein level by western blotting and/or mass spectrometry-based proteomics.

Apart from the HSPs, it is also clear that certain proteasomal subunits were upregulated in response to the BTZ treatment at 12 and 24 h (**Supplemental Table 1**), including orthologs of

various regulatory subunits belonging to the 19S proteasome cap (Smp_072340, 052870 and 119310), as well as the α and β subunits (Smp_121430 and 067890) that make up the 20S core. This increased synthesis of the proteasome is consistent with the literature for cancer cells (**102,103**) and the fruit-fly (**104**) as part of the unfolded-protein stress response. As found for the SmHSPs, the *S. mansoni* proteasome subunit genes are well represented across the different developmental stages of the parasite (**Table 2**).

A detailed analysis of the 205 genes exclusive to either the 12 and 24 h time points (**Figure 6**) is beyond the scope of this thesis. Nonetheless, it is worth noting that a number of genes were upregulated only after the 12 h time point, for example, Smp_085740, (abl-interactor (Abi) protein; 1.7-fold upregulated), Smp_011600 (connector enhancer of kinase suppressor of ras 2 (CNKSR2); 2.2-fold upregulated) and Smp_140630 (TELO2-interacting protein 1 (Tti); 1.9-fold upregulated (**Supplemental Table 1**). Abi family proteins regulate cytoskeletal dynamics, including cytokinesis, and transport carrier biogenesis (**105**). CNKSR2 is a scaffold protein that mediates the mitogen-activated protein kinase pathways that are responsible for cell differentiation, proliferation and metabolism (**106**). Tti is part of a complex of proteins that engages the serine/threonine protein kinase, MTOR, a key regulator of transcription and translation that controls cell growth and survival (**107-109**).

Upregulation of these proteins may represent an 'early' active rescue response by the parasite to compensate for proteasome blockade but this rescue is then replaced by terminal responses such as apoptosis, including the expression of caspases (**102**) which our lab has previously measured after 24 h in the presence of 1 μM BTZ (**49**). Of note, many of the genes associated with this early 12 h response encode protein kinases and phosphatases, which are

druggable (**110**), and one or more of which may prove useful as a novel anti-schistosomal drug target, including in combination with a proteasome inhibitor.

Genes of interest that are only upregulated after the 24 h timepoint (**Figure 6**) include Smp_210400 (ATP-dependent Clp protease proteolytic subunit; 1.6-fold upregulated), Smp_011960 (Inositol-pentakisphosphate 2-kinase; 2.6-fold upregulated) and Smp_172200 (tyrosine kinase; 2.4-fold upregulated). ATP-dependent Clp protease proteolytic subunit is found in the mitochondrion and shares considerable structural and functional similarities to the proteasome (**111,112**), including β5-like chymotrypsin activity that contributes to degrading misfolded proteins. Its upregulation may be a compensatory action to deal with increasing levels of misfolded proteins in the mitochondrion as a result of proteasome blockade.

Inositol-pentakisphosphate 2-kinase catalyzes the last step in inositol 1,2,3,4,5,6-hexakisphosphate (phytic acid) synthesis in mammals (**113**). Because phytic acid is involved in a broad range of cellular functions, including RNA export, DNA repair, signaling, endocytosis and cell vesicle movement (**114,115**), its upregulation suggests a response by the worm to maintain homeostasis in one or more of these functions.

Lastly, tyrosine kinases mediate signal transduction, proliferation, differentiation and migration of cells by phosphorylating tyrosine residues (**116**). In current cancer treatments, research has shown that the inhibition of both tyrosine kinases and the proteasome can counter the resistance developed in some leukemias to targeting tyrosine kinases alone (**117**). Given the upregulation of tyrosine kinases in *S. mansoni* after exposure to BTZ, future experiments could consider a combination of proteasome and tyrosine kinase inhibitors to induce cell death as has been reported for some leukemias (**117**).

RNA-Seq is a powerful tool to generate a snapshot of the transcriptional state of a cell or organism as it responds to internal or external stimuli (**118-120**). The data generated by RNA-Seq must be validated, however, by a secondary method such as qPCR (**121**). Thus, in completion of the second aim of my thesis, the qPCR data displayed in **Figure 7** for the nine targeted genes of interest agree well with the fold-upregulation of the same genes as measured by RNA-Seq, suggesting that the RNA-Seq data, as a whole, are accurate. Generation of those qPCR data required considerable effort in first conducting the necessary bioinformatics to choose putative primers pairs and then ensuring their optimal efficiency. On average, for each gene target, three to five qPCR test runs were needed before optimal efficiency was obtained.

6. Conclusion

The research presented here is part of an ongoing project by my lab to investigate the proteasome as drug target for treatment of schistosomiasis. Using RNA-Seq, my thesis has facilitated an initial understanding of some key gene transcripts upregulated by adult *S. mansoni* in response to its exposure to 1 μM BTZ after 12 h and 24 h – conditions that impede parasite motility and induce caspase activity (the latter of which is a hallmark of proteasome blockade (**49**)). Understanding which genes are upregulated in response to BTZ offers possibilities for new drug interventions, either independently or combined with proteasome inhibition (**53,54,122**). My research also developed a qPCR assay for nine example genes to confirm the RNA-Seq data. Lastly, the developmental-stage expression profile of some key upregulated genes, such as the HSPs and proteasome subunits, demonstrated their broad distribution across the *S. mansoni* lifecycle.

Supplemental Methods.

1.0 Integrative analysis and Venn diagram generation

Fold expression and gene name data from RNA-Seq runs were pasted into Excel to compare commonly expressed genes between gene groups using Venn diagrams. Gene lists were obtained via ROSALIND (OnRamp™) which identified genes significantly upregulated (fold change ≥1.5; P-Adj ≤ 0.05), compared to DMSO-treated controls. Each list was pasted into Excel columns "A" and "C", respectively. To compare these lists and generate data for the Venn diagrams, "two-way" comparisons were generated using two formulae employing the "FILTER" function in Excel. This function was used to compare columns "A" and "C," and identify common Smp_IDs for the different drug treatments. The "FILTER" function identifies a matching range of values based on the supplied criteria. The following "filters" (shown below), were entered in "Excel Macros". These filters were then used to select genes that were commonly found across both BTZ 12 and 24 h treatments.

FILTER I. =FILTER(A2:A301, 1-COUNTIF(C2:C301, A2:A301))

FILTER II. *=FILTER(C2:C301, 1-COUNTIF(A2:A301, C2:C301))*

The result of the subtraction of FILTER II – FILTER I yields the number of common genes between both gene lists: BTZ 12 (12 h) and BTZ 24 (24 h).

The information generated in Excel was used to create Venn Diagrams in RStudio ™ (2020, MA, USA). Two-way Venn Diagrams of BTZ 12 and BTZ 24 were generated as in the following example:

```
grid.newpage()
draw.pairwise.venn(2467, 1590, 990, category = c("BTZ 12", "BTZ 24"), lty = rep("blank",
   2), fill = c("red", "yellow"), alpha = rep(0.5, 2), cat.pos = c(0,
   0), cat.dist = rep(0.025, 2))
```

The raw numerical data generated from this code was inputted into the software, My Draw (https://www.mydraw.com/templates-venn-diagram-index) to generate the Venn diagram. This output was redrawn in PowerPoint (**Figure 6**).

Supplemental Tables

Supplemental Table 1. Top 300 most upregulated genes after 1 μM BTZ treatment for 12 h and/or 24 h.

		BTZ 12 h		BTZ 24 h	
Gene Identifier	Gene Name	Fold Change	P-adj value	Fold Change	P-adj value
Smp_106930*	Heat shock 70 kDa protein homolog	12.96	9.98E-44	13.19	2.73E-15
Smp_049250*	Heat shock protein-HSP20/alpha crystallin family	8.93	1.89E-69	11.48	7.74E-11
Smp_049240	Heat-shock protein beta-1 (HspB1) (Heat shock 27 kDa protein) (HSP 27)	7.05	3.33E-15	4.24	5.48E-04
Smp_072330	Heat shock protein	6.60	2.46E-234	4.28	9.59E-08
Smp_149750	Vacuolar sorting associated	5.48	2.80E-14	7.62	3.86E-09
Smp_151640	Insulin-like growth factor	4.94	1.43E-20	2.52	1.35E-02
Smp_040680	Cytoplasmic dynein light chain	4.78	5.41E-89	4.72	5.47E-09
Smp_049300	Major egg antigen	4.43	2.17E-09	5.89	2.60E-05
Smp_200900	Uncharacterized protein	4.36	3.14E-48	3.81	4.08E-06
Smp_185680	Major egg antigen	4.22	1.11E-08	5.58	5.11E-05
Smp_011150	Taspase-1 (T02 family)	3.54	4.35E-48	3.78	2.33E-06
Smp_069130	Heat shock protein 70 (Hsp70)-4_ putative	3.32	1.90E-121	2.85	8.00E-06
Smp_172460	Kruppel-like factor 11, partial	3.18	3.14E-27	3.20	1.76E-04
Smp_131000	Harp (Smarcal1)-related	3.18	7.07E-64	2.42	7.91E-06
Smp_156450	Uncharacterized protein	3.05	5.58E-81	3.08	1.98E-05
Smp_146450	Octopamine receptor	2.96	1.07E-20	3.05	4.04E-04
Smp_123260*	Ubiquitin 1	2.95	1.34E-43	5.08	1.29E-06
Smp_008545	Heat shock protein HSP60_ putative	2.93	4.60E-174	2.94	4.17E-06
Smp_081600	Alkylated DNA repair protein alkB 4	2.90	9.06E-09	2.56	3.75E-03
Smp_197790	Alpha-ketoglutarate-dependent dioxygenase alkB 4	2.83	4.83E-08	2.87	1.58E-03
Smp_059660	Metallo-beta-lactamase domain-containing protein 1	2.78	1.47E-115	3.05	6.09E-05
Smp_202770	Uncharacterized protein	2.70	4.86E-24	2.42	1.01E-03
Smp_072460	Phosphomevalonate kinase	2.64	1.79E-06	4.01	3.26E-05
Smp_064860	Heat shock protein 70 (Hsp70)-interacting protein	2.59	1.26E-134	2.26	2.02E-04
Smp_043580	Histone-lysine n-methyltransferase_ setb1	2.59	3.43E-24	3.24	1.20E-04
Smp_036090	Ankyrin repeat and LEM domain-containing protein isoform 1	2.59	1.61E-51	2.25	5.25E-04
Smp_189960	Nuclear pore complex protein Nup153	2.57	9.96E-30	3.04	1.21E-06
Smp_050470	Transducin beta-like protein 3	2.56	1.34E-43	3.06	2.94E-06
Smp_091810	Nuclear pore complex protein Nup153	2.53	3.57E-51	2.84	2.29E-05
Smp_210170	RNA polymerase II subunit B1 CTD phosphatase Rpap2 mRNA	2.51	3.61E-26	2.72	1.41E-04

Supplemental Table 1. (Cont.)

Smp_021830	Phosphatidylserine decarboxylase proenzyme 1	2.45	7.10E-25	2.42	1.81E-04
Smp_004680	Interferon-related developmental regulator-related	2.44	3.67E-79	2.36	1.18E-03
Smp_180190	Uncharacterized protein	2.39	5.54E-19	3.69	2.94E-06
Smp_176110	Leucine rich repeat-containing domain	2.38	3.80E-11	4.86	1.29E-06
Smp_165970	Acidic fibroblast growth factor intracellular binding protein	2.38	4.38E-29	2.18	2.28E-03
Smp_129320	Cell division control protein_ putative	2.38	1.45E-48	2.43	1.21E-04
Smp_167110	Invadolysin (M08 family)	2.37	1.47E-04	3.12	4.71E-04
Smp_144300	Tns1 protein	2.34	1.92E-11	2.59	1.25E-03
Smp_043360	Uncharacterized protein	2.33	1.14E-05	2.96	2.32E-04
Smp_163100	High-affinity cgmp-specific 3_5-cyclic phosphodiesterase	2.29	1.79E-21	2.36	9.39E-04
Smp_205200	Octopamine receptor	2.28	1.07E-03	2.28	1.16E-02
Smp_162990	tRNA pseudouridine synthase 2	2.24	4.09E-17	2.87	7.67E-05
Smp_154030	Uncharacterized protein	2.22	5.69E-16	2.23	1.77E-03
Smp_061570	Lung cancer metastasis-related (Lcmr1) protein	2.19	1.80E-20	2.35	1.04E-03
Smp_168000	Monocarboxylate transporter	2.17	1.06E-18	2.67	2.33E-06
Smp_151320	Tpx2 protein	2.16	1.16E-03	3.63	9.65E-04
Smp_186940	Uncharacterized protein	2.15	3.01E-10	2.23	5.61E-03
Smp_156400	Cytochrome P450	2.15	1.83E-04	3.37	1.45E-04
Smp_076450	Uncharacterized protein	2.10	2.90E-12	2.94	3.57E-05
Smp_136950	Protein SREK1IP1	2.10	1.39E-12	2.25	1.68E-03
Smp_127700	Protein prenyltransferase alpha subunit repeat-containing protein 1	2.09	2.17E-08	2.53	2.28E-03
Smp_019190	Step II splicing factor slu7_ putative	2.07	4.57E-45	2.62	2.86E-04
Smp_121140	Uncharacterized protein	2.07	6.31E-14	2.34	1.37E-03
Smp_130220	Uncharacterized protein	2.06	1.03E-12	2.17	1.99E-04
Smp_119120	Oxygenase-related	2.06	4.22E-05	3.28	2.25E-04
Smp_005910	Tyrosine phosphatase prl	2.05	5.16E-38	2.19	3.47E-04
Smp_025670	Zinc finger C2H2-type domain-containing protein	1.98	6.88E-23	2.63	7.46E-05
Smp_153560	Ring finger protein B (Protein rngB)	1.97	1.70E-32	2.23	2.81E-03
Smp_152520	Cpg binding protein	1.97	1.08E-17	2.47	7.38E-05
Smp_152440	HIV Tat-specific factor 1-like protein	1.95	1.36E-25	2.22	2.96E-04
Smp_159120	Family C48 unassigned peptidase (C48 family)	1.94	1.44E-26	2.23	7.63E-04
Smp_076630	Nonsense-mediated mRNA decay protein	1.93	1.01E-21	2.37	1.16E-04
Smp_130840	Regulatory NSL complex subunit 3	1.93	3.26E-12	2.51	1.97E-07
Smp_133770	Glutamine synthetase bacteria	1.92	1.26E-02	5.61	5.51E-06
Smp_027340	Insulin-inducedprotein	1.91	3.00E-21	2.80	8.77E-04

Supplemental Table 1. (Cont.)

Smp_148120	Ctd sr related rna binding protein	1.91	7.79E-10	2.18	7.14E-04
Smp_128400	Uncharacterized protein	1.91	5.49E-15	2.23	6.99E-04
Smp_158280	Zinc finger protein_ putative	1.91	2.55E-06	2.51	2.32E-03
Smp_101650	Long-chain-fatty-acid-CoA ligase	1.88	1.05E-02	2.30	1.03E-02
Smp_070340	Histone-arginine methyltransferase 1.3	1.87	3.26E-26	2.31	1.16E-04
Smp_010800	S-adenosylmethionine-dependent methyltransferase related	1.86	2.35E-07	2.54	1.06E-03
Smp_065160	Taz protein (Tafazzin)	1.85	6.55E-06	2.21	2.91E-03
Smp_178920	Trna(5-methylaminomethyl-2-thiouridylate)-methy lt ransferase	1.85	1.40E-06	2.63	7.63E-04
Smp_138220	DFDF motif	1.85	4.54E-34	2.20	6.64E-04
Smp_130330	Uncharacterized protein	1.84	2.09E-08	3.45	2.33E-06
Smp_140690	Dna-directed RNA polymerase I subunit	1.81	3.58E-11	2.59	8.74E-05
Smp_022140	Serine/threonine-protein kinase rio1 (Rio kinase 1)_ putative	1.80	4.11E-10	2.73	3.26E-05
Smp_171150*	Shk1 kinase-binding protein	1.80	3.04E-15	2.33	3.49E-04
Smp_053470	Nucleolar protein NOP56	1.79	2.07E-10	2.83	1.52E-04
Smp_124170	Dynein heavy chain	1.78	8.02E-07	2.31	6.87E-04
Smp_090370	Nuclear pore complex protein Nup50	1.78	1.44E-08	2.33	5.97E-04
Smp_019040	Transcription factor lbp1_cp2	1.78	1.85E-17	2.53	2.81E-04
Smp_018570	Serine-rich repeat protein 2	1.78	9.62E-10	2.49	9.65E-04
Smp_040190	Serine/threonine kinase	1.78	2.25E-14	2.25	3.00E-03
Smp_145650	Forkhead box protein K2	1.76	4.23E-10	2.23	1.40E-03
Smp_171070	Cell cycle control protein cwf22	1.75	2.09E-17	2.35	1.93E-04
Smp_082660	Transcription intermediary factor 1-related	1.74	8.62E-13	2.18	6.87E-04
Smp_158740	Uncharacterized protein	1.74	7.43E-17	2.59	4.71E-04
Smp_168130	Phosphatase and actin regulator_ putative	1.73	2.78E-06	2.45	2.35E-03
Smp_134290	Serine-rich repeat protein	1.72	1.42E-15	2.22	3.47E-04
Smp_140760	Uncharacterized protein	1.71	1.69E-15	2.21	2.87E-03
Smp_137800	Uncharacterized protein	1.70	2.22E-04	2.45	1.16E-04
Smp_157800	Dead box ATP-dependent RNA helicase	1.68	3.05E-08	2.42	3.68E-04
Smp_194580	Edp1-related	1.67	3.17E-12	2.40	3.33E-04
Smp_085790	Uncharacterized protein	1.67	1.26E-08	2.23	1.54E-03
Smp_200180	Cytoplasmic Dynein Light Chain	3.42	1.09E-71	1.95	1.95E-03
Smp_150990	Cationic amino acid transporter	2.83	5.87E-12	2.14	1.09E-02
Smp_210980	Protein phosphatase 1	2.75	1.55E-68	1.95	3.57E-05
Smp_201060	Probable dynein light chain	2.60	1.25E-45	N/A	N/A
Smp_051580	Uncharacterized protein	2.58	6.29E-07	2.14	3.49E-02
Smp_083080	Uncharacterized protein	2.57	3.01E-92	2.17	4.14E-04

Supplemental Table 1. (Cont.)

Smp_174890	TATA box-binding protein-associated factor RNA polymerase I subunit A	2.55	1.69E-40	2.03	3.97E-03
Smp_127490	Blooms syndrome DNA helicase	2.53	5.70E-22	N/A	N/A
Smp_072340*	26s protease regulatory subunit 6b	2.46	1.13E-52	1.94	1.84E-03
Smp_042270	26S protease regulatory subunit 6a_ putative	2.36	3.70E-68	1.69	1.60E-03
Smp_042390	2-deoxyglucose-6-phosphate phosphatase	2.34	5.67E-19	1.81	4.48E-03
Smp_009580	Ubiquitin	2.31	8.00E-114	1.95	1.37E-03
Smp_004780	Immunophilin	2.29	2.93E-126	1.90	3.65E-04
Smp_115060	KRR1 small subunit processome component-like protein	2.26	3.19E-15	2.12	9.99E-04
Smp_175250	26S proteasome regulatory subunit rpn2_putative	2.22	1.61E-55	N/A	N/A
Smp_011600	Connector enhancer of kinase suppressor of ras 2	2.21	1.55E-20	N/A	N/A
Smp_160200	Smad nuclear interacting protein	2.21	3.44E-17	1.66	3.97E-02
Smp_065120	Deoxyhypusine synthase	2.19	1.52E-24	2.06	6.78E-04
Smp_020920	Dnaj homolog subfamily B member 4	2.19	2.29E-67	1.96	6.87E-04
Smp_079750	Methyltransferase	2.18	1.65E-21	1.92	9.23E-04
Smp_142770	Importin-beta 2	2.16	5.21E-54	2.06	3.30E-04
Smp_072720	Zinc finger protein_ putative	2.16	2.00E-80	2.09	1.75E-03
Smp_122550	Gtp binding protein	2.15	3.50E-41	1.89	2.17E-03
Smp_150780	Queuine tRNA-ribosyltransferase	2.14	8.43E-30	2.12	1.03E-03
Smp_144090	Hyperparathyroidism homolog	2.12	2.81E-33	1.69	1.24E-02
Smp_061590	Nonsense-mediated mRNA decay protein 1 (Rent1)_putative	2.10	1.81E-25	N/A	N/A
Smp_159810	MEG-2 (ESP15) family	2.08	3.14E-03	N/A	N/A
Smp_097380	Groes chaperonin	2.07	1.30E-46	2.00	2.91E-03
Smp_159510	Uncharacterized protein	2.06	2.09E-18	1.96	6.68E-03
Smp_025130	Rna binding motif protein	2.05	5.33E-18	N/A	N/A
Smp_088550	Rrm/rnp domain	2.04	4.65E-33	2.06	1.70E-03
Smp_061650	26S proteasome subunit S9_ putative	2.03	2.63E-52	1.57	2.74E-04
Smp_051280	Smg-7 (Suppressor with morphological effect on genitalia protein 7)_ putative	2.03	1.62E-42	1.89	6.02E-03
Smp_070070	Fip1-like 1 protein	2.02	2.82E-16	1.72	2.09E-02
Smp_193150	Uncharacterized protein	2.00	9.35E-07	2.06	3.56E-03
Smp_080740	Translation initiation factor	2.00	2.20E-03	N/A	N/A
Smp_150910	UBP1-associated proteins 1C	2.00	1.07E-09	1.89	1.68E-03
Smp_196220	Zinc finger protein	2.00	2.63E-18	1.62	4.48E-02
Smp_178740	Tesmin-related	1.98	2.06E-12	1.64	6.43E-03
Smp_035540	Uncharacterized protein	1.98	7.98E-22	2.04	8.46E-04
Smp_093800	Mitochondrial import inner membrane translocase subunit TIM21	1.98	6.44E-12	2.02	3.46E-03

Supplemental Table 1. (Cont.)

Smp_094770	DNAj-like subfamily B member	1.98	7.89E-16	N/A	N/A
Smp_134870	Early growth response protein	1.98	8.29E-15	2.07	6.22E-03
Smp_080370	Uncharacterized protein	1.97	2.02E-62	1.89	2.99E-03
Smp_021980	-	1.97	8.68E-23	1.70	1.28E-03
Smp_067900	Cdc37-related	1.97	1.91E-37	1.75	2.63E-03
Smp_173840	26S protease regulatory subunit_ putative	1.96	2.53E-57	N/A	N/A
Smp_058620	Serine/threonine kinase	1.96	2.32E-28	1.97	1.17E-03
Smp_026160	Growth hormone inducible transmembrane protein	1.95	8.54E-73	2.07	1.37E-03
Smp_167070	Leishmanolysin-2 (M08 family)	1.95	1.77E-06	1.88	2.01E-02
Smp_076890	Splicing factor 3A subunit 2	1.94	1.74E-03	N/A	N/A
Smp_128990	Biorientation of chromosomes in cell division protein	1.94	7.15E-13	N/A	N/A
Smp_145680	Pleckstrin y protein	1.93	2.87E-20	2.04	5.02E-03
Smp_084940	Gtp-binding protein rit	1.93	4.46E-56	1.76	3.02E-03
Smp_052870*	26s proteasome non-ATPase regulatory subunit	1.93	8.90E-40	1.55	2.55E-04
Smp_047740	26S proteasome non-ATPase regulatory subunit_putative	1.92	2.60E-30	N/A	N/A
Smp_101890	Protein lin-54-like protein	1.92	3.12E-06	N/A	N/A
Smp_085310	26S proteasome regulatory subunit S3_ putative	1.92	7.59E-36	N/A	N/A
Smp_140630	TELO2-interacting protein 1-like protein	1.92	3.64E-05	N/A	N/A
Smp_142710	Fkbp-rapamycin associated protein	1.92	2.83E-29	1.72	6.27E-03
Smp_169770	Glycosylphosphatidylinositol anchor attachment 1 protein	1.91	1.63E-22	1.77	3.30E-04
Smp_102240*	Upf3 regulator of nonsense transcripts-like protein	1.91	1.74E-23	2.06	1.16E-04
Smp_009340	Ribosomal RNA assembly protein	1.91	5.25E-12	1.95	3.86E-03
Smp_015840	Zinc finger protein	1.89	1.30E-29	2.03	9.39E-04
Smp_157370	Serine/threonine kinase	1.89	1.18E-12	1.81	3.30E-02
Smp_067890*	Proteasome subunit alpha type	1.88	1.20E-28	1.54	3.14E-03
Smp_133380	Serine/threonine-protein phosphatase PGAM5	1.88	2.79E-08	1.70	3.55E-03
Smp_121430	Proteasome subunit beta type	1.88	7.00E-39	1.54	2.48E-03
Smp_154780	S-adenosylmethionine-dependent methyltransferase related	1.88	2.06E-18	1.97	2.20E-03
Smp_025680	COP9 signalosome complex subunit 8	1.87	8.44E-15	1.76	1.80E-03
Smp_176290	Tyrosyl-tRNA synthetase_ putative	1.87	2.05E-14	1.77	6.70E-03
Smp_162050	Uncharacterized protein	1.87	1.55E-23	2.09	7.63E-04
Smp_020800	Cysteine and histidine-rich domain (Chord)-containing_ zinc binding protein_ putative	1.87	9.52E-34	1.84	1.14E-03
Smp_017070	26s protease regulatory subunit S10b	1.86	6.65E-46	N/A	N/A
Smp_077000	Uncharacterized protein	1.86	7.67E-04	1.94	7.09E-03

Supplemental Table 1. (Cont.)

Smp_128420	Protein CASC3	1.86	1.86E-24	1.77	6.70E-03
Smp_197730	Rrm-containing protein seb-4_ putative	1.85	6.99E-17	1.68	1.54E-02
Smp_155210	Uncharacterized protein	1.84	2.84E-12	N/A	N/A
Smp_174960	Merlin/moesin/ezrin/radixin	1.84	2.12E-22	N/A	N/A
Smp_074060	Uncharacterized protein	1.84	1.50E-12	1.55	1.33E-02
Smp_164970	Protein Kinase	1.84	1.71E-06	1.84	5.00E-03
Smp_033050	Dna topoisomerase type I	1.84	4.22E-44	2.14	5.16E-04
Smp_209050	Peptidyl-prolyl cis-trans isomerase-like 4. ppil4	1.84	2.34E-17	N/A	N/A
Smp_045750	Cak assembly factor	1.83	1.92E-13	N/A	N/A
Smp_096210	Uncharacterized protein	1.83	1.37E-21	N/A	N/A
Smp_132170	Jumonji domain containing protein	1.83	1.61E-15	1.75	9.24E-03
Smp_125050	Hepatoma derived growth factor_ putative	1.83	1.62E-18	N/A	N/A
Smp_180210	WW domain-containing adapter protein isoform 2	1.83	5.65E-20	1.53	3.48E-02
SmtRNA_00024_Gln.1	-	1.83	2.80E-02	N/A	N/A
Smp_135510	NAALADASE L peptidase (M28 family)	1.82	4.88E-18	1.71	1.68E-03
Smp_067440	Oligodendrocyte transcription factor 2	1.82	1.99E-07	1.99	2.57E-03
Smp_034490	Proteasome subunit beta type	1.82	1.02E-27	N/A	N/A
Smp_187960	WW domain-containing adapter protein	1.81	3.85E-12	N/A	N/A
Smp_210480	Aminopeptidase P homologue (M24 family)	1.81	6.52E-12	1.81	2.03E-03
Smp_002160	DNA methyltransferase 1-associated protein 1	1.81	1.01E-19	2.09	5.58E-04
Smp_104630	Wdr4-prov protein	1.81	2.06E-13	1.99	5.25E-04
Smp_157520	Transcription factor HIVEP3	1.81	7.41E-18	1.69	1.81E-02
Smp_084540	G patch domain-containing protein 1 (Evolutionarily conserved G-patch domain containing protein)	1.81	2.08E-32	1.96	7.78E-04
Smp_009530	Deoxycytidylate deaminase	1.81	2.69E-08	1.82	8.26E-04
Smp_177080	Alpha-1_3-mannosyltransferase	1.81	2.13E-23	1.80	1.65E-03
Smp_133470	Ribonucleoprotein-related	1.81	1.65E-13	2.10	1.24E-03
Smp_039640	Retinoblastoma binding protein	1.80	3.78E-28	N/A	N/A
Smp_127630	Transketolase	1.80	9.05E-04	1.70	1.61E-02
Smp_077010	Uncharacterized protein	1.80	8.55E-08	1.80	2.92E-02
Smp_162600	HEAT repeat-containing protein 1	1.80	1.97E-23	2.06	1.27E-03
Smp_103090	Histone-lysine N-methyltransferase SETD2	1.80	4.59E-29	N/A	N/A
Smp_130270	Uncharacterized protein	1.80	7.68E-07	2.05	2.30E-03
Smp_132180	Uncharacterized protein	1.79	6.16E-16	2.03	1.68E-03
Smp_035480	Arginine and glutamate-rich protein 1	1.79	2.40E-21	1.91	7.34E-03
Smp_078310	Ran-binding protein	1.79	4.25E-19	1.58	1.53E-02

Supplemental Table 1. (Cont.)

Smp_023990	Transcriptional repressor protein yy (Yin and yang) (Delta transcription factor)	1.78	1.29E-14	N/A	N/A
Smp_145430	Cement precursor 3B variant 2	1.78	4.66E-12	N/A	N/A
Smp_160550	Dyp-type peroxidase_ putative	1.78	2.12E-05	N/A	N/A
Smp_123340	Uncharacterized protein	1.78	4.02E-11	2.04	9.72E-04
Smp_021960	Uncharacterized protein	1.78	2.21E-11	N/A	N/A
Smp_131650	Telomerase-binding protein EST1A	1.77	2.19E-21	N/A	N/A
Smp_181090	Rna (Guanine-9-) methyltransferase domain containing	1.77	1.39E-11	1.88	3.00E-03
Smp_093950	Family C85 unassigned peptidase (C85 family)	1.77	2.64E-28	1.59	5.98E-03
Smp_180040	Phosphoglycerate mutase	1.77	3.78E-24	N/A	N/A
Smp_199850	Peter pan-related	1.76	1.05E-03	2.12	1.16E-02
Smp_138680	DNAj homolog subfamily C member_ putative	1.76	4.83E-29	1.78	3.22E-03
Smp_092280	Proteasome subunit alpha 3 (T01 family)	1.76	1.95E-24	N/A	N/A
Smp_181290	Large subunit ribosomal protein L28	1.76	5.75E-08	N/A	N/A
Smp_212500	Peter pan-related	1.76	7.65E-12	2.13	6.99E-04
Smp_074620	Nucleoside diphosphate hydrolase_ putative	1.75	3.63E-07	N/A	N/A
Smp_198750	Pinn_ putative	1.75	1.91E-19	2.04	9.41E-04
Smp_145880	Abhydrolase domain-containing protein 4 (S33 family)	1.75	3.69E-08	2.14	2.48E-03
Smp_144740	4.1 G protein_ putative	1.75	4.20E-02	N/A	N/A
Smp_059910	Uncharacterized protein	1.75	1.17E-11	1.73	1.87E-03
Smp_038700	Uncharacterized protein	1.75	9.94E-27	N/A	N/A
Smp_175920	Uncharacterized protein	1.75	2.09E-12	2.03	8.80E-03
Smp_148330	DENN domain-containing protein 1	1.75	1.60E-12	N/A	N/A
Smp_024970	Ccr4 not-related	1.75	5.26E-22	N/A	N/A
Smp_142950	DNA-directed RNA polymerase III subunit RPC5	1.74	4.47E-18	1.86	6.99E-04
Smp_018620	Paraplegin (M41 family)	1.74	5.82E-18	1.57	2.38E-03
Smp_044810	Zinc finger CCCH domain-containing protein isoform 1	1.74	5.16E-20	1.78	5.55E-03
Smp_210180	Ubiquitin-like protein 5	1.74	4.75E-06	1.67	1.56E-02
Smp_156710	Phosphatidylinositol-4-phosphate-5-kinase_putativ e	1.74	3.53E-06	1.58	3.96E-03
Smp_145740	Cdc6_ putative	1.74	2.42E-10	N/A	N/A
ENSRNA022728962	U1 spliceosomal RNA	1.74	4.46E-02	N/A	N/A
Smp_074500	Proteasome subunit beta 2 (T01 family)	1.74	1.21E-22	1.55	2.24E-03
Smp_170540	Arginine-glutamic acid dipeptide repeats protein	1.74	1.02E-34	1.95	2.42E-03
Smp_005080	Nucleolar protein nol1/nop2	1.73	7.88E-11	1.67	1.25E-02
Smp_164860	Metallophosphoesterase 1	1.73	1.03E-09	N/A	N/A
Smp_022660	Wd-repeat protein	1.73	5.53E-25	1.96	5.25E-04

Supplemental Table 1. (Cont.)

Smp_192000	Queuine tRNA-ribosyltransferase	1.73	2.75E-10	1.59	9.15E-03
Smp_159870	Uncharacterized protein	1.73	1.91E-14	1.77	4.17E-03
Smp_076040	DIF_3	1.73	3.59E-29	1.82	2.65E-03
Smp_076230	Proteasome subunit alpha type	1.73	1.05E-33	N/A	N/A
Smp_055340	Lin-9	1.73	5.90E-18	N/A	N/A
Smp_168940	Nad dependent epimerase/dehydratase	1.73	5.24E-06	2.05	3.20E-03
Smp_143920	Integrator complex subunit 9	1.73	1.11E-11	1.90	1.05E-03
Smp_194620	Methyltransferase_ putative	1.72	3.82E-07	1.78	1.68E-03
Smp_164770	Apg5-related	1.72	1.98E-19	1.70	4.43E-03
Smp_007510	Protein kinase	1.72	7.74E-17	N/A	N/A
Smp_022330	Dnaj homolog subfamily B member 2_ 6_ 8	1.72	6.55E-46	1.61	1.31E-03
Smp_210680	Suppression of tumorigenicity	1.72	9.20E-13	1.81	4.21E-03
Smp_019820	Uncharacterized protein	1.72	9.78E-09	1.81	3.14E-03
Smp_138920	Cop9 signalosome complex subunit	1.72	6.67E-18	1.81	1.19E-03
Smp_015780	Atpase n2b	1.71	3.01E-12	2.00	1.82E-03
Smp_204730	Uncharacterized protein	1.71	3.41E-16	1.72	2.79E-03
Smp_035090	Hepatoma up-regulated protein	1.71	1.78E-20	2.11	5.67E-04
Smp_104370	CCR4-NOT Transcription complex subunit 4	1.71	2.95E-04	N/A	N/A
Smp_012150	Zinc finger C4H2 domain-containing protein	1.71	2.96E-22	2.05	1.31E-03
Smp_170950	Transferase CAF17-like protein	1.71	4.02E-06	N/A	N/A
Smp_157910	Uncharacterized protein	1.71	4.51E-17	1.68	1.06E-02
Smp_129720	Fuse-binding protein-interacting repressor siahbp1_ putative	1.71	2.69E-17	1.84	1.60E-03
Smp_176550	Lipoyltransferase 2_ mitochondrial	1.71	3.90E-12	N/A	N/A
Smp_146570	Histidyl-tRNA synthetase-related	1.71	7.11E-16	1.65	1.12E-02
Smp_126720	Pre-mRNA splicing factor ISY1-like protein	1.71	1.42E-16	1.72	2.17E-03
Smp_125340	Hepatoma derived growth factor	1.70	3.85E-14	N/A	N/A
Smp_160870	Aaa family ATPase	1.70	3.75E-12	2.00	1.34E-03
Smp_198870	Long-chain-fatty-acid--CoA ligase	1.70	9.63E-15	N/A	N/A
Smp_050700	Phosphatidylethanolamine-binding protein	1.70	2.82E-15	1.75	1.41E-03
Smp_045600	Golgin subfamily A member 6 6	1.70	6.13E-04	1.87	2.27E-03
Smp_127580	DIS3-like exonuclease 2	1.70	4.81E-13	2.02	6.36E-04
Smp_035360	Nucleolar protein 14	1.70	7.31E-09	N/A	N/A
Smp_090340	Uncharacterized protein	1.70	1.43E-04	1.58	2.08E-02
Smp_038940	Mrna (Guanine-7-)methyltransferase	1.69	9.89E-09	N/A	N/A
Smp_036500	CAR; nuclear receptor nhr-48	1.69	1.29E-21	1.80	6.63E-03
Smp_054300	Alpha(1_3)fucosyltransferase	1.69	1.74E-03	N/A	N/A

Supplemental Table 1. (Cont.)

Smp_005900	Bcl2-associated athanogene	1.69	2.42E-36	1.77	1.85E-03
Smp_157530	Transcription factor HIVEP3	1.69	4.67E-07	1.97	1.58E-03
Smp_045070	U3 Small Nucleolar RNA-associated protein 15	1.69	1.38E-11	1.68	9.43E-03
Smp_085740	Abl-binding protein-related	1.69	1.77E-19	N/A	N/A
Smp_154640	SWI/SNF-related	1.68	6.27E-10	N/A	N/A
Smp_166550	Translation initiation factor 2b_ delta subunit_putative	1.68	1.32E-14	1.80	1.73E-03
Smp_138050	Polypyrimidine tract binding protein_ putative	1.68	1.64E-32	1.69	7.09E-03
Smp_207030	Gtpase activating protein-related	1.68	6.56E-14	N/A	N/A
Smp_149350	Uro-adherence factor A	1.68	7.81E-14	1.97	5.24E-03
Smp_142300	Polypyrimidine tract binding protein	1.68	1.73E-18	N/A	N/A
Smp_072900	Hsp90 co-chaperone (Tebp)_ putative	1.68	1.59E-36	1.66	9.39E-04
Smp_152010	Uncharacterized protein	1.68	3.81E-22	1.83	2.94E-03
Smp_073410	Proteasome subunit beta type	1.68	8.32E-36	N/A	N/A
Smp_211200	Williams-beuren syndrome critical region protein_ putative	1.68	1.16E-08	N/A	N/A
Smp_083680	Nucleolar protein 53	1.67	9.51E-14	1.54	1.21E-02
Smp_087220	Microprocessor complex subunit DGCR8	1.67	1.11E-11	1.62	2.98E-03
Smp_176670	Histone H2A	1.67	1.25E-03	N/A	N/A
Smp_039390	Distal membrane-arm assembly complex protein	1.67	7.44E-09	1.70	5.55E-03
Smp_164850	Metallophosphoesterase 1	1.67	2.55E-04	N/A	N/A
Smp_153190	Integrator complex subunit	1.67	1.40E-14	1.56	3.02E-02
Smp_092170	Regulation of nuclear pre-mRNA domain-containing protein 1A	1.67	2.50E-10	2.06	3.26E-03
Smp_062420	Heat shock protein 70 (Hsp70)-interacting protein	1.67	4.31E-56	N/A	N/A
Smp_073680	Tata-box binding protein	1.67	4.95E-17	N/A	N/A
Smp_130020	Uncharacterized protein	1.67	3.89E-03	N/A	N/A
Smp_210400	ATP-dependent Clp protease proteolytic subunit	N/A	N/A	1.58	0.02989
SmtRNA_02247_Gln_TTG.1.1	-	N/A	N/A	6.31	1.44E-07
SmtRNA_02231_Gln_TTG.1.1	-	N/A	N/A	6.07	2.33E-06
Smp_048050	Alpha crystallin A chain	N/A	N/A	6.03	1.97E-07
Smp_049230	Heat shock protein hsp16	N/A	N/A	5.61	1.97E-07
SmtRNA_00711_Pseudo_TTG.1.1	-	N/A	N/A	5.35	1.46E-05
SmtRNA_01532_Gln_TTG.1.1	-	N/A	N/A	5.07	1.16E-04
Smp_138080	MEG-3 (Grail) family	N/A	N/A	4.92	1.24E-04

Supplemental Table 1. (Cont.)

SmtRNA_00559_Gln_TTG.1.1	-	N/A	N/A	4.87	7.83E-05
SmtRNA_00178_Gln_TTG.1.1	-	N/A	N/A	4.82	1.25E-04
SmtRNA_00186_Pseudo_TTG.1.1	-	N/A	N/A	4.60	2.49E-04
Smp_138070	MEG-3 (Grail) family	N/A	N/A	4.56	3.24E-04
Smp_138060	MEG-3 (Grail) family	N/A	N/A	4.47	4.51E-04
SmtRNA_01408_Pseudo_TTG.1.1	-	N/A	N/A	4.44	3.33E-04
SmtRNA_02198_Glu_TTC.1.1	-	N/A	N/A	4.43	2.02E-04
SmtRNA_00233_Gln_TTG.1.1	-	N/A	N/A	4.42	4.60E-04
Smp_003600	Natterin-4	N/A	N/A	4.41	3.47E-04
SmtRNA_02435_Gln_TTG.1.1	-	N/A	N/A	4.38	3.82E-04
SmtRNA_01400_Pseudo_TTG.1.1	-	N/A	N/A	4.07	7.63E-04
SmtRNA_00556_Gln_TTG.1.1	-	N/A	N/A	4.06	6.11E-04
SmtRNA_01995_Gln_TTG.1.1	-	N/A	N/A	3.95	3.24E-04
SmtRNA_02285_Pseudo_TTG.1.1	-	N/A	N/A	3.80	1.44E-03
SmtRNA_02391_Pseudo_CGA.1.1	-	N/A	N/A	3.79	1.17E-03
ENSRNA022734481	TRNA-Pro for anticodon AGG	N/A	N/A	3.72	1.68E-03
Smp_160160	Sialin (Solute carrier family 17 member 5) (Sodium/sialic acid cotransporter) (Ast) (Membrane glycoprotein hp59)	N/A	N/A	3.71	5.71E-05
SmtRNA_01540_Gln_TTG.1.1	-	N/A	N/A	3.70	6.99E-04
SmtRNA_00502_Gln_TTG.1.1	-	N/A	N/A	3.68	1.03E-03
SmtRNA_02277_Gln_TTG.1.1	-	N/A	N/A	3.67	1.83E-03
SmtRNA_00149_Gln_TTG.1.1	-	N/A	N/A	3.67	1.04E-03

Supplemental Table 1. (Cont.)

SmtRNA_00150_Pseudo_TTG.1.1	-	N/A	N/A	3.64	4.30E-04
SmtRNA_00139_Pseudo_TTG.1.1	-	N/A	N/A	3.63	1.90E-03
SmtRNA_00551_Pseudo_TTG.1.1	-	N/A	N/A	3.62	1.57E-03
SmtRNA_01333_Pseudo_TTG.1.1	-	N/A	N/A	3.58	1.21E-03
Smp_181330	Uncharacterized protein	N/A	N/A	3.54	2.42E-03
Smp_056680	Cercarial elastase (S01 family)	N/A	N/A	3.53	2.47E-03
SmtRNA_00443_Gln_TTG.1.1	-	N/A	N/A	3.52	2.32E-03
SmtRNA_00239_Gln_TTG.1.1	-	N/A	N/A	3.52	1.54E-03
SmtRNA_00984_Gln_TTG.1.1	-	N/A	N/A	3.41	3.22E-03
Smp_178990	Uncharacterized protein	1.62	3.25E-12	3.40	4.80E-05
Smp_203150	Uncharacterized protein	N/A	N/A	3.37	6.04E-04
SmtRNA_02082_Gln_TTG.1.1	-	N/A	N/A	3.34	3.47E-03
SmtRNA_01659_Gln_TTG.1.1	-	N/A	N/A	3.28	4.22E-03
SmtRNA_02255_Gln_TTG.1.1	-	N/A	N/A	3.27	3.60E-03
SmtRNA_01944_Gln_TTG.1.1	-	N/A	N/A	3.26	4.25E-03
Smp_188430	Glutathione synthetase	N/A	N/A	3.26	2.62E-04
Smp_131330	Uncharacterized protein	N/A	N/A	3.19	4.86E-03
SmtRNA_01727_Pseudo_TTG.1.1	-	N/A	N/A	3.16	4.92E-03
SmtRNA_01379_Gln_TTG.1.1	-	N/A	N/A	3.16	5.45E-03
Smp_205180	Lipoate-protein ligase	N/A	N/A	3.14	5.05E-03
SmtRNA_01606_Pseudo_CGA.1.1	-	N/A	N/A	3.14	5.79E-03
Smp_177650	Glutathione synthase	N/A	N/A	3.11	2.62E-04
Smp_079960	Tubulin beta chain	N/A	N/A	3.09	4.95E-03
SmtRNA_02251_Pseudo_TTG.1.1	-	N/A	N/A	3.09	6.40E-03

Supplemental Table 1. (Cont.)

SmtRNA_01393_Gln_TTG.1.1	-	N/A	N/A	3.09	6.47E-03
SmtRNA_00134_Gln_TTG.1.1	-	N/A	N/A	3.08	6.55E-03
SmtRNA_00962_Gln_TTG.1.1	-	N/A	N/A	3.06	5.97E-03
SmtRNA_00684_Pseudo_TTG.1.1	-	N/A	N/A	3.05	6.57E-03
Smp_180660	Uncharacterized protein	N/A	N/A	3.01	4.96E-03
SmtRNA_01445_Gln_TTG.1.1	-	N/A	N/A	3.00	7.67E-03
SmtRNA_00941_Gln_TTG.1.1	-	N/A	N/A	2.99	7.61E-03
Smp_125890	DNA photolyase	1.65	9.06E-09	2.97	3.32E-05
SmtRNA_01473_Gln_TTG.1.1	-	N/A	N/A	2.96	5.79E-03
SmtRNA_01046_Pseudo_ATG.1.1	-	N/A	N/A	2.95	9.72E-04
Smp_033000	Calcium-binding protein	N/A	N/A	2.93	4.00E-03
ENSRNA022733861	TRNA-Leu for anticodon UAG	N/A	N/A	2.92	9.51E-03
SmtRNA_00635_Pseudo_GTG.1.1	-	N/A	N/A	2.89	9.41E-03
Smp_205910	WGS project CABG00000000 data_ supercontig 0881_ strain Puerto Rico	1.55	2.36E-05	2.86	8.33E-04
SmtRNA_00248_Pseudo_CGA.1.1	-	N/A	N/A	2.85	1.11E-02
SmtRNA_01873_Pseudo_TTG.1.1	-	N/A	N/A	2.82	9.84E-03
Smp_100310	Hexaprenyldihydroxybenzoate methyltransferase, mitochondrial	N/A	N/A	2.81	1.16E-02
Smp_123390	Requim_ req/dpf2_	N/A	N/A	2.80	1.41E-04
Smp_055850	Threonyl-tRNA synthetase_ cytoplasmic_	N/A	N/A	2.80	8.79E-03
Smp_062900	Peroxiredoxin_ Prx4	N/A	N/A	2.79	6.04E-03
SmtRNA_02047_Gln_TTG.1.1	-	N/A	N/A	2.79	1.03E-02
SmtRNA_01735_Pseudo_TTG.1.1	-	N/A	N/A	2.78	1.26E-02
SmtRNA_00414_Pseudo_TTG.1.1	-	N/A	N/A	2.76	1.38E-02
ENSRNA022738551	TRNA-Glu for anticodon UUC	N/A	N/A	2.76	1.40E-02

Supplemental Table 1. (Cont.)

SmtRNA_01512_Pseudo_TTG.1.1	-	N/A	N/A	2.74	1.29E-02
Smp_075030	Myotrophin	1.63	7.32E-06	2.73	7.68E-04
Smp_149680	Early growth response protein_	N/A	N/A	2.72	6.45E-04
Smp_127610	Mername-AA213 peptidase (M14 family)	N/A	N/A	2.71	1.11E-02
Smp_188200	DM9 domain containing protein	N/A	N/A	2.69	1.18E-02
Smp_087330	Uncharacterized protein	1.53	1.84E-05	2.68	2.32E-04
Smp_021070	Gtp-binding protein-animal	N/A	N/A	2.66	7.67E-05
Smp_011960	Inositol-pentakisphosphate 2-kinase	N/A	N/A	2.66	6.87E-04
SmtRNA_02084_Gln_TTG.1.1	-	N/A	N/A	2.64	1.74E-02
Smp_123970	Uncharacterized protein	N/A	N/A	2.61	2.00E-02
SmtRNA_02094_Gln_TTG.1.1	-	N/A	N/A	2.59	2.08E-02
SmtRNA_02117_Pseudo_TTG.1.1	-	N/A	N/A	2.59	2.08E-02
ENSRNA022728979	U6 spliceosomal RNA	N/A	N/A	2.57	2.01E-02
Smp_043610	Pre-mRNA-splicing regulator female-lethal(2)D	N/A	N/A	2.56	6.24E-04
SmtRNA_00091_Pseudo_TTG.1.1	-	N/A	N/A	2.56	2.13E-02
ENSRNA022734732	TRNA-Ser for anticodon UGA	N/A	N/A	2.55	1.86E-02
SmtRNA_01190_Pseudo_TTA.1.1	-	N/A	N/A	2.54	2.34E-02
SmtRNA_01092_Gln_TTG.1.1	-	N/A	N/A	2.54	2.33E-02
SmtRNA_01029_Pseudo_CGA.1.1	-	N/A	N/A	2.53	2.10E-02
SmtRNA_02022_Gln_TTG.1.1	-	N/A	N/A	2.53	2.30E-02
Smp_200560	Histone H2B	N/A	N/A	2.52	6.56E-03
SmtRNA_02356_Pseudo_TTG.1.1	-	N/A	N/A	2.52	2.14E-02
SmtRNA_02195_Pseudo_TTG.1.1	-	N/A	N/A	2.52	2.20E-02
Smp_122770	Cap-specific mRNA (nucleoside-2'-O-)methyltransferase 1	N/A	N/A	2.52	1.20E-02
Smp_168250	Uncharacterized protein	N/A	N/A	2.51	2.54E-02
SmtRNA_02187_Pseudo_TGA.1.1	-	N/A	N/A	2.51	2.52E-02

Supplemental Table 1. (Cont.)

SmtRNA_01625_Pseudo_TTG.1.1	-	N/A	N/A	2.51	2.33E-02
Smp_200090	Leucine zipper and W2 domains 1 BZW1	N/A	N/A	2.50	1.31E-03
Smp_134480	Proline-rich protein PRCC	1.64	8.04E-09	2.49	1.52E-04
SmtRNA_02327_Gln_TTG.1.1	-	N/A	N/A	2.49	2.69E-02
Smp_172200	Tyrosine kinase	N/A	N/A	2.49	2.32E-04
Smp_196900	Uncharacterized protein	N/A	N/A	2.49	1.34E-02
ENSRNA022733349	TRNA-Ser for anticodon AGA	N/A	N/A	2.48	2.31E-02
Smp_033590	RING finger protein 113A	N/A	N/A	2.48	2.63E-04
SmtRNA_02329_Gln_TTG.1.1	-	N/A	N/A	2.47	2.38E-02
Smp_043200	Serine/threonine-protein kinase rio2 (Rio kinase 2)	N/A	N/A	2.47	3.65E-04
Smp_191380	RUNX1 Translocation partner 1 RUNX1T1	N/A	N/A	2.47	2.81E-02
Smp_170020	Neuropeptide receptor	N/A	N/A	2.47	2.13E-03
SmtRNA_02341_Gln_TTG.1.1	-	N/A	N/A	2.46	2.87E-02
Smp_173260	TIMELESS-interacting protein	N/A	N/A	2.46	1.01E-03
Smp_185340	Alpha(1,3) fucosyltransferase	1.60	4.51E-02	2.45	6.45E-03
Smp_129510	UPF0046-like	1.65	1.73E-03	2.45	1.01E-03
Smp_149690	Uncharacterized protein	N/A	N/A	2.45	1.16E-02
Smp_156060	Pre-mRNA-splicing factor ATP-dependent RNA helicase PRP16	1.51	2.31E-10	2.45	4.62E-04
SmtRNA_00638_Gln_TTG.1.1	-	N/A	N/A	2.44	3.05E-02
Smp_105070	Uncharacterized protein	1.66	3.64E-09	2.44	1.81E-04
SmtRNA_00449_Pseudo_TTG.1.1	-	N/A	N/A	2.44	2.58E-02
Smp_122090	Transient receptor potential cation channel	N/A	N/A	2.44	2.63E-04
Smp_179720	Oxysterol-binding protein	1.61	2.41E-07	2.44	3.05E-04
Smp_160170	Cilia and flagella associated protein	1.65	1.37E-03	2.44	2.91E-04
Smp_126380	Eyes absent	N/A	N/A	2.43	3.13E-02
Smp_201810	Uncharacterized protein	N/A	N/A	2.43	1.74E-03
Smp_150440	Tubulin-specific chaperone E	1.61	1.73E-06	2.43	1.82E-03
SmtRNA_00379_Gln_TTG.1.1	-	N/A	N/A	2.42	3.20E-02
SmtRNA_00404_Gln_TTG.1.1	-	N/A	N/A	2.42	3.17E-02

Supplemental Table 1. (Cont.)

Smp_194390	Suppressor of cytokine signaling	N/A	N/A	2.40	4.30E-04
Smp_013570	Uncharacterized protein	1.64	3.31E-03	2.40	1.17E-03
SmtRNA_00175_Gln_TTG.1.1	-	N/A	N/A	2.39	3.34E-02
SmtRNA_01896_Gln_CTG.1.1	-	N/A	N/A	2.39	3.09E-02
Smp_122340	Kelch-like protein	N/A	N/A	2.39	1.63E-03
Smp_090890	Serine/threonine protein kinase	1.56	8.51E-09	2.38	1.07E-03
SmtRNA_02191_Gln_TTG.1.1	-	N/A	N/A	2.38	3.39E-02
Smp_076710	Uncharacterized protein	N/A	N/A	2.38	2.42E-03
SmtRNA_02040_Pseudo_TTG.1.1	-	N/A	N/A	2.37	3.59E-02
Smp_153240	Fibrocystin-L	N/A	N/A	2.36	2.92E-02
sma.28s-95.1	-	N/A	N/A	2.36	3.09E-02
SmtRNA_01994_Gln_TTG.1.1	-	N/A	N/A	2.36	3.53E-02
Smp_098980	Hsda/sda1_	1.53	2.72E-09	2.36	4.80E-05
SmtRNA_01174_Pseudo_TTG.1.1	-	N/A	N/A	2.36	3.38E-02
Smp_142820	Retinol Dehydrogenase 12 isoform 2	1.51	3.50E-02	2.36	7.74E-03
SmtRNA_00465_Pseudo_TTG.1.1	-	N/A	N/A	2.35	3.79E-02
Smp_092930	Uncharacterized protein	1.52	2.08E-05	2.35	6.28E-04
Smp_169340	Coiled-coil domain-containing protein 58	N/A	N/A	2.35	5.61E-04
Smp_211160	ATP-dependent RNA helicase_	1.56	2.17E-03	2.35	7.78E-04
Smp_176760	Metaxin_	N/A	N/A	2.34	6.58E-04
SmtRNA_00562_Gln_TTG.1.1	-	N/A	N/A	2.34	4.01E-02
SmtRNA_01862_Pseudo_TTG.1.1	-	N/A	N/A	2.33	3.50E-02
ENSRNA022728978	U6 spliceosomal RNA	1.65	2.96E-02	2.33	3.80E-02
Smp_053420	Fermitin family 1	1.54	1.98E-24	2.33	6.92E-04
SmtRNA_01581_Pseudo_TTG.1.1	-	N/A	N/A	2.33	4.05E-02
Smp_180610	Protein AF-17	N/A	N/A	2.32	7.28E-03
Smp_012010	Forkhead transcription factor	N/A	N/A	2.31	3.65E-03
Smp_122730	Cap-specific (nucleoside-2'-o-)-methyltransferase 1	N/A	N/A	2.31	4.38E-04

Supplemental Table 1. (Cont.)

Smp_164740	Zinc finger protein_	N/A	N/A	2.30	3.90E-02
SmtRNA_01320_Pseudo_TTG.1.1	-	N/A	N/A	2.29	4.33E-02
SmtRNA_00439_Gln_TTG.1.1	-	N/A	N/A	2.29	3.93E-02
Smp_151110	Uncharacterized protein	1.57	1.54E-04	2.29	4.51E-04
Smp_000110	Similar to elongation factor Tu GTP binding domain containing 1 isoform 6-related	1.54	8.49E-09	2.29	4.52E-04
SmtRNA_02071_Gln_TTG.1.1	-	N/A	N/A	2.28	2.96E-02
Smp_077740	Uncharacterized protein	N/A	N/A	2.28	2.76E-02
Smp_159620	BTB/POZ domain-containing protein KCTD20	N/A	N/A	2.28	2.34E-03
SmtRNA_01728_Gln_TTG.1.1	-	N/A	N/A	2.28	4.67E-02
Smp_047860	Ribosomal pseudouridine synthase	N/A	N/A	2.28	7.94E-04
Smp_058680	Ribosome biogenesis regulatory protein_	1.52	1.74E-06	2.28	5.20E-04
Smp_169300	Transcription initiation factor tfiid 55 kD subunit-related	1.63	3.84E-10	2.27	8.33E-04
SmtRNA_01694_Pseudo_TTG.1.1	-	N/A	N/A	2.27	4.74E-02
SmtRNA_02272_Gln_TTG.1.1	-	N/A	N/A	2.27	3.90E-02
Smp_143440	Uncharacterized protein	1.64	6.56E-07	2.27	7.01E-04
Smp_021130	Uncharacterized protein	N/A	N/A	2.26	1.08E-03
SmtRNA_00299_Gln_TTG.1.1	-	N/A	N/A	2.26	4.83E-02
Smp_054120	Ribosome biogenesis protein NSA2 homologue	N/A	N/A	2.26	1.81E-04
SmtRNA_01441_Gln_TTG.1.1	-	N/A	N/A	2.25	4.17E-02
Smp_030350	Subfamily S1A unassigned peptidase (S01 family)	N/A	N/A	2.24	4.01E-02
Smp_090520	Purine nucleoside phosphorylase	N/A	N/A	2.24	2.10E-03
Smp_173090	Eyes absent homolog	N/A	N/A	0.00	0.00E+00
Smp_202620	Transposon Curupira-2	N/A	N/A	2.24	4.99E-02
SmtRNA_00434_Gln_TTG.1.1	-	N/A	N/A	2.22	4.03E-02
Smp_160590	Uncharacterized protein	N/A	N/A	2.22	3.16E-03
Smp_069910	28S ribosomal protein S35 (mitochondrial mRNA)	N/A	N/A	2.22	6.99E-04

Supplemental Table 1. (Cont.)

SmtRNA_01068_Gln_TTG.1.1	-	N/A	N/A	0.00	0.00E+00
SmtRNA_00321_Gln_TTG.1.1	-	N/A	N/A	0.00	0.00E+00
Smp_180990	Dachshund homolog	1.62	1.18E-05	2.21	2.54E-04
SmtRNA_01923_Pseudo_TTG.1.1	-	N/A	N/A	0.00	0.00E+00
Smp_177240	Twinkle protein (mitochondria mRNA)	N/A	N/A	2.21	3.05E-03
Smp_034300	Transcription factor ETV6	N/A	N/A	2.20	3.29E-03
Smp_133310	Uncharacterized protein	N/A	N/A	2.20	1.77E-03
Smp_073510	Protein kinase	N/A	N/A	2.20	6.99E-04
Smp_048620	Exosome complex exonuclease rrp45 (Polymyositis/scleroderma autoantigen 1) (Ribosomal rna processing protein 45)	N/A	N/A	2.20	9.17E-05
Smp_100030	Ribosome biogenesis protein BMS1	1.55	3.46E-08	2.20	2.42E-03
Smp_034310	Uncharacterized protein	N/A	N/A	2.19	8.13E-03
SmtRNA_01744_Glu_CTC.1.1	-	N/A	N/A	0.00	0.00E+00
ENSRNA022759130	U2 spliceosomal RNA	N/A	N/A	0.00	0.00E+00
Smp_201310	Alpha-ketoglutarate-dependent dioxygenase alkB 7 (mitochondrial mRNA)	N/A	N/A	2.18	3.06E-02
SmtRNA_01806_Pseudo_TTG.1.1	-	N/A	N/A	0.00	0.00E+00
SmtRNA_01903_Gln_TTG.1.1	-	N/A	N/A	2.18	3.82E-02
Smp_119310*	Proteasome subunit α-type	1.54	1.70E-20	1.59	4.17E-03
Smp_130700	Uncharacterized protein	N/A	N/A	2.18	2.25E-03
SmtRNA_02102_Pseudo_CGA.1.1	-	N/A	N/A	2.18	4.95E-02
Smp_002010	Nep1	N/A	N/A	2.17	4.51E-04
Smp_127100	YrdC domain-containing protein	N/A	N/A	2.17	1.57E-03

N/A; gene was not found for that time point

* ; part of qPCR gene set.

Colors: any color means manually characterized following the Methods in Section 3.10:

Blue; both BLASTn and BLASTp returned the same characterization

Green; only BLASTp provided the characterization

Orange; only BLASTn provided the characterization

Yellow; both BLASTn and BLASTp returned different characterizations, but BLASTp was chosen due to the search result having the greater Max Score

Pink; both BLASTn and BLASTp returned different characterizations, but BLASTn was chosen due to the search result having the greater Max Score

Supplemental Figures

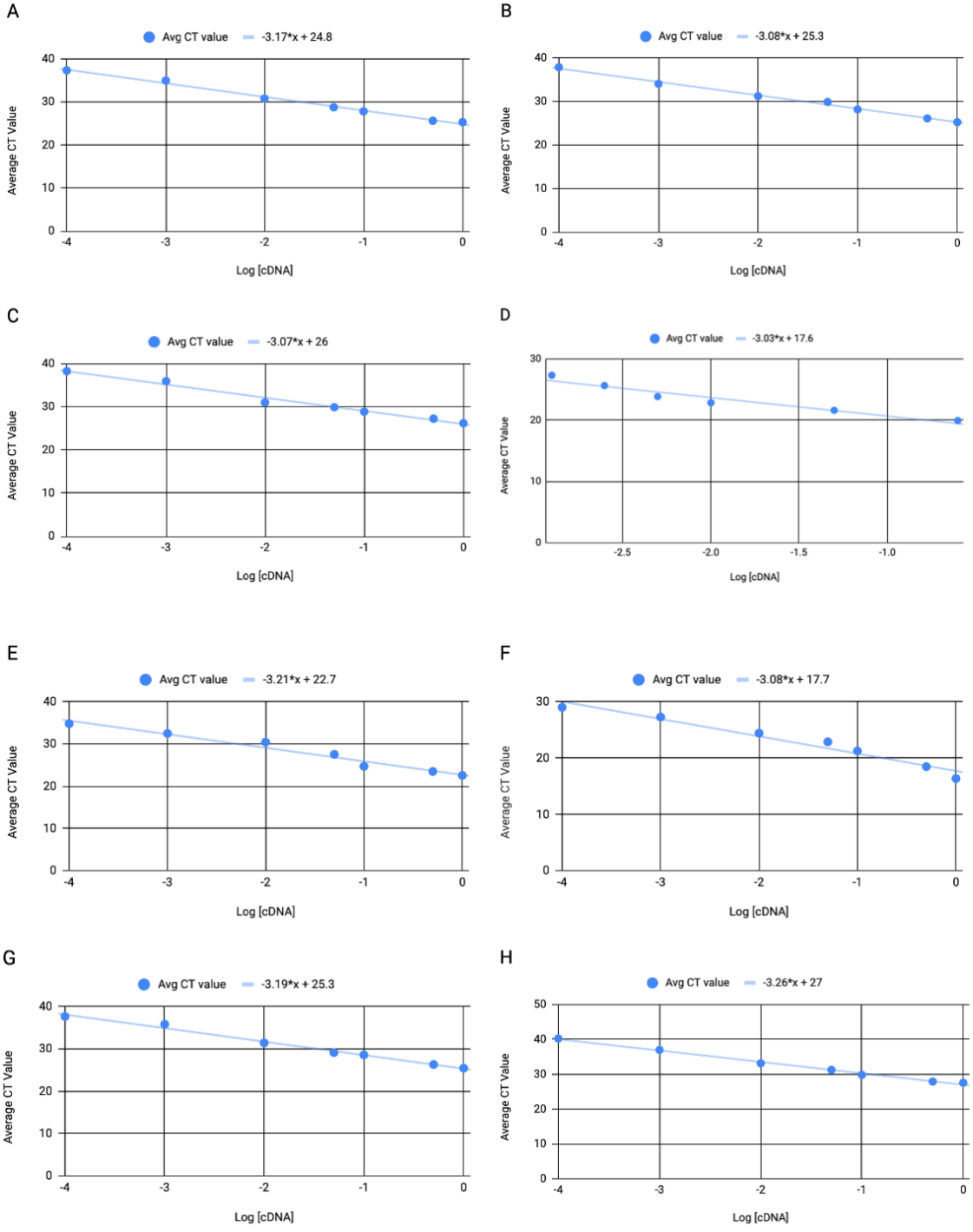

Supplemental Figure 1. (Cont.)

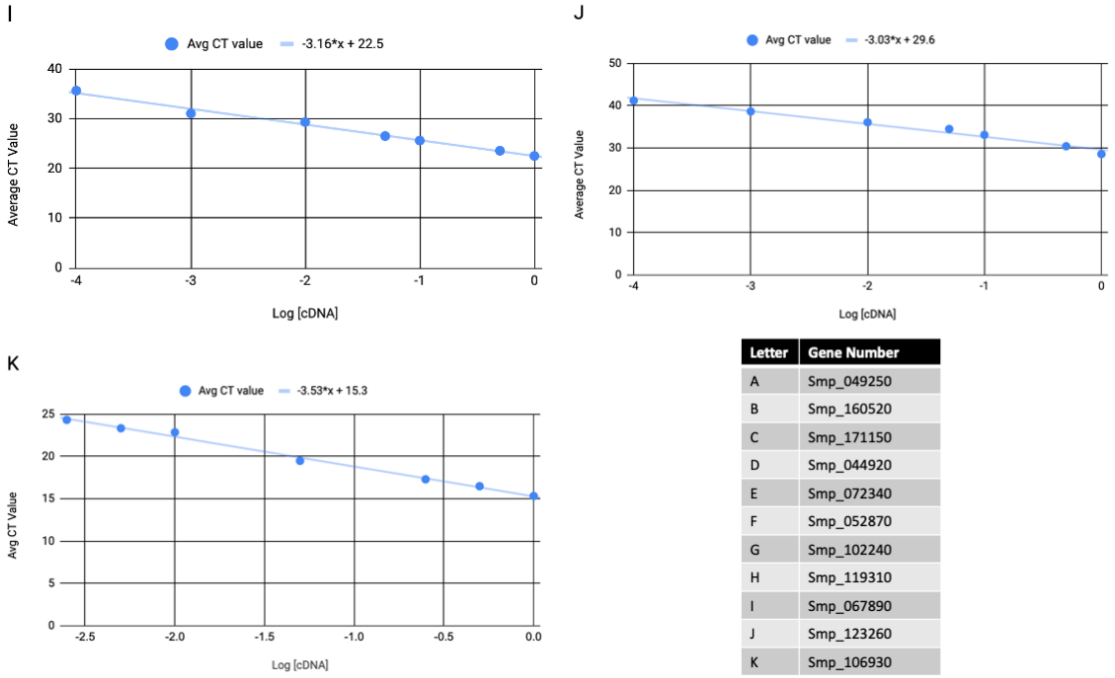

Letter	Gene Number
A	Smp_049250
B	Smp_160520
C	Smp_171150
D	Smp_044920
E	Smp_072340
F	Smp_052870
G	Smp_102240
H	Smp_119310
I	Smp_067890
J	Smp_123260
K	Smp_106930

Supplemental Figure 1. Primer efficiency optimization curves for the 11 genes of interest. Each primer set is shown with the resulting slope being utilized to calculate its efficiency. Each of these datapoints was obtained using a dilution series to test primer binding. The formula used to calculate primer efficiency was $10^{[(-1/slope)-1]} * 100\%$. Each graph is labeled with a letter and the table shows the corresponding gene.

References

1. Colley, D. G., Bustinduy, A. L., Secor, W. E., & King, C. H. (2014). Human schistosomiasis. *The Lancet*, *383*(9936), 2253–2264. https://doi.org/10.1016/S0140-6736(13)61949-2

2. Wu, G. Y., & Halim, M. H. (2000). Schistosomiasis: Progress and problems. In *World Journal of Gastroenterology* (Vol. 6, Issue 1, pp. 12–19). WJG Press. https://doi.org/10.3748/wjg.v6.i1.12

3. Khiani, V., & King, C. H. (2009). Schistosomiasis: Schistosoma haematobium. In *Medical Parasitology* (pp. 129–135). CRC Press. https://doi.org/10.1201/9781498713672-29

4. King, C. H. (2011). *SCHISTOSOMIASIS: CHALLENGES AND OPPORTUNITIES*. https://www.ncbi.nlm.nih.gov/books/NBK62510/

5. McManus, D. P., Dunne, D. W., Sacko, M., Utzinger, J., Vennervald, B. J., & Zhou, X. N. (2018). Schistosomiasis. *Nature Reviews Disease Primers*, *4*(1), 1–19. https://doi.org/10.1038/s41572-018-0013-8

6. Berriman, Matthew, Brian J. Haas, Philip T. LoVerde, R. Alan Wilson, Gary P. Dillon, Gustavo C. Cerqueira, Susan T. Mashiyama, Bissan Al-Lazikani, Luiza F. Andrade, Peter D. Ashton, Martin A. Aslett, Daniella C. Bartholomeu, Gaelle Blandin, Conor R. Caffrey, Avril Coghlan, Richard Coulson, Tim A. Day, Art Delcher, Ricardo DeMarco, Appolinaire Djikeng, Tina Eyre, John A. Gamble, Elodie Ghedin, Yong Gu, Christiane Hertz-Fowler, Hirohisha Hirai, Yuriko Hirai, Robin Houston, Alasdair Ivens, David A. Johnston, Daniela Lacerda, Camila D. Macedo, Paul McVeigh, Zemin Ning, Guilherme Oliveira, John P. Overington, Julian Parkhill, Mihaela Pertea, Raymond J. Pierce, Anna V. Protasio, Michael A. Quail, Marie-Adèle Rajandream, Jane Rogers, Mohammed Sajid, Steven L. Salzberg, Mario Stanke, Adrian R. Tivey, Owen White, David L. Williams, Jennifer Wortman, Wenjie Wu, Mostafa Zamanian, Adhemar Zerlotini, Claire M. Fraser-Liggett, Barclay G. Barrell, and Najib M. El-Sayed. "The Genome of the Blood Fluke Schistosoma Mansoni." *Nature* 460.7253 (2009): 352-58. Print.

7. Wu, W., Feng, A., & Huang, Y. (2015). Research and control of advanced schistosomiasis japonica in China. In *Parasitology Research* (Vol. 114, Issue 1, pp. 17–27). Springer Verlag. https://doi.org/10.1007/s00436-014-4225-x

8. Nelwan, M. L. (2019). Schistosomiasis: Life Cycle, Diagnosis, and Control. In *Current Therapeutic Research - Clinical and Experimental* (Vol. 91, pp. 5–9). Excerpta Medica Inc. https://doi.org/10.1016/j.curtheres.2019.06.001

9. *CDC - Schistosomiasis - Biology*. (n.d.). Retrieved January 13, 2021, from https://www.cdc.gov/parasites/schistosomiasis/biology.html

10. Pallangyo, P., Bhalia, S., Simelane, N. N., Lyimo, F., Swai, H. J., Mkojera, Z. S., Hemed, N. R., Misidai, N., Millinga, J., & Janabi, M. (2020). Massive Bilateral Hydroureteronephrosis and End-Stage Renal Disease Ensuing From Chronic

Schistosomiasis: A Case Report. Journal of Investigative Medicine High Impact Case Reports, 8. https://doi.org/10.1177/2324709620910912

11. What is schistosomiasis? | Facts | yourgenome.org. (n.d.). Retrieved February 11, 2021, from https://www.yourgenome.org/facts/what-is-schistosomiasis

12. Protasio, Anna V., Isheng J. Tsai, Anne Babbage, Sarah Nichol, Martin Hunt, Martin A. Aslett, Nishadi De Silva, Giles S. Velarde, Tim J. Anderson, Richard C. Clark, Claire Davidson, Gary P. Dillon, Nancy E. Holroyd, Philip T. LoVerde, Christine Lloyd, Jacquelline McQuillan, Guilherme Oliveira, Thomas D. Otto, Sophia J. Parker-Manuel, Michael A. Quail, R. Alan Wilson, Adhemar Zerlotini, David W. Dunne, and Matthew Berriman. "A Systematically Improved High Quality Genome and Transcriptome of the Human Blood Fluke Schistosoma Mansoni." *PLoS Neglected Tropical Diseases* 6.1 (2012). Print.

13. Nation, C. S., Da'dara, A. A., Marchant, J. K., & Skelly, P. J. (2020). Schistosome migration in the definitive host. In PLoS Neglected Tropical Diseases (Vol. 14, Issue 4, pp. 1–12). Public Library of Science. https://doi.org/10.1371/journal.pntd.0007951

14. Popiel, I., & Basch, P. F. (1984). Reproductive development of female Schistosoma mansoni (Digenea: Schistosomatidae) following bisexual pairing of worms and worm segments. Journal of Experimental Zoology, 232(1), 141–150. https://doi.org/10.1002/jez.1402320117

15. Pearce, E. J., & Huang, S. C. C. (2015). The metabolic control of schistosome egg production. Cellular Microbiology, 17(6), 796–801. https://doi.org/10.1111/cmi.12444

16. Kunz, W. (2001). Schistosome male-female interaction: induction of germ-cell differentiation. In Trends in Parasitology (Vol. 17, Issue 5, pp. 227–231). Elsevier. https://doi.org/10.1016/S1471-4922(01)01893-1

17. Yu-Jin Lee. (n.d.). Retrieved January 13, 2021, from https://web.stanford.edu/group/parasites/ParaSites2010/Yu-Jin_Lee/LeeY.ParaSite.original_japonicum_transmission_snails.htm

18. Haeberlein, S., & Haas, W. (2008). Chemical attractants of human skin for swimming Schistosoma mansoni cercariae. Parasitology Research, 102(4), 657–662. https://doi.org/10.1007/s00436-007-0807-1

19. Hall, S. C., & Kehoe, E. L. (1970). Case reports. Prolonged survival of Schistosoma japonicum. *California Medicine*, *113*(2), 75–77. https://www.ncbi.nlm.nih.gov/pmc/articles/PMC1501527/

20. Payet, B., Chaumentin, G., Boyer, M., Amaranto, P., Lemonon-Meric, C., & Lucht, F. (2006). Prolonged latent schistosomiasis diagnosed 38 years after infestation in a HIV patient. Scandinavian Journal of Infectious Diseases, 38(6–7), 572–575. https://doi.org/10.1080/00365540500444660

21. U Olveda, D. (2013). Bilharzia: Pathology, Diagnosis, Management and Control. Tropical Medicine & Surgery, 01(04), 135. https://doi.org/10.4172/2329-9088.1000135

22. Jenkins, S. J., Hewitson, J. P., Jenkins, G. R., & Mountford, A. P. (2005). Modulation of the host's immune response by schistosome larvae. In Parasite Immunology (Vol. 27, Issues 10–11, pp. 385–393). Europe PMC Funders. https://doi.org/10.1111/j.1365-3024.2005.00789.x

23. CDC - Schistosomiasis - Disease. (n.d.). Retrieved February 15, 2021, from https://www.cdc.gov/parasites/schistosomiasis/disease.html

24. Gray, D. J., Ross, A. G., Li, Y. S., & McManus, D. P. (2011). Diagnosis and management of schistosomiasis. In BMJ (Vol. 342, Issue 7807). BMJ Publishing Group. https://doi.org/10.1136/bmj.d2651

25. Holmen, S. D., Kleppa, E., Lillebø, K., Pillay, P., Van Lieshout, L., Taylor, M., Albregtsen, F., Vennervald, B. J., Onsrud, M., & Kjetland, E. F. (2015). The first step toward diagnosing female genital schistosomiasis by computer image analysis. American Journal of Tropical Medicine and Hygiene, 93(1), 80–86. https://doi.org/10.4269/ajtmh.15-0071

26. Wan, H., Lei, D., & Mao, Q. (2009). Cerebellar Schistosomiasis: A Case Report with Clinical Analysis. The Korean Journal of Parasitology, 47(1), 53. https://doi.org/10.3347/kjp.2009.47.1.53

27. Engels, D., Hotez, P. J., Ducker, C., Gyapong, M., Bustinduy, A. L., Secor, W. E., Harrison, W., Theobald, S., Thomson, R., Gamba, V., Masong, M. C., Lammie, P., Govender, K., Mbabazi, P. S., & Malecela, M. N. (2020). Integration of prevention and control measures for female genital schistosomiasis, hiv and cervical cancer. Bulletin of the World Health Organization, 98(9), 615–624. https://doi.org/10.2471/BLT.20.252270

28. Schistosomiasis (Bilharzia). (n.d.). Retrieved January 15, 2021, from https://www.who.int/health-topics/schistosomiasis#tab=tab_1

29. Aruleba, R. T., Adekiya, T. A., Oyinloye, B. E., Masamba, P., Mbatha, L. S., Pretorius, A., & Kappo, A. P. (2019). PZQ Therapy: How Close are we in the Development of Effective Alternative Anti-schistosomal Drugs? Infectious Disorders - Drug Targets, 19(4), 337–349. https://doi.org/10.2174/1871526519666181231153139

30. CDC Map. (n.d.). Retrieved January 15, 2021, from https://www.cdc.gov/travel-static/yellowbook/2018/map_3-12.pdf

31. Mafe, M. A., Appelt, B., Adewale, B., Idowu, E. T., Akinwale, O. P., Adeneye, A. K., Manafa, O. U., Sulyman, M. A., Akande, O. D., & Omotola, B. D. (2005). Effectiveness of different approaches to mass delivery of praziquantel among school-aged children in rural communities in Nigeria. Acta Tropica, 93(2), 181–190. https://doi.org/10.1016/j.actatropica.2004.11.004

32. Munisi, D. Z., Buza, J., Mpolya, E. A., Angelo, T., & Kinung'hi, S. M. (2017). The Efficacy of Single-Dose versus Double-Dose Praziquantel Treatments on Schistosoma mansoni Infections: Its Implication on Undernutrition and Anaemia among Primary Schoolchildren in Two On-Shore Communities, Northwestern Tanzania. BioMed Research International, 2017. https://doi.org/10.1155/2017/7035025

33. Li, E. Y., Gurarie, D., Lo, N. C., Zhu, X., & King, C. H. (2019). Improving public health control of schistosomiasis with a modified WHO strategy: a model-based comparison study. *The Lancet Global Health*, *7*(10), e1414–e1422. https://doi.org/10.1016/S2214-109X(19)30346-8

34. Caffrey, C. R. (2015). Schistosomiasis and its treatment. In Future Medicinal Chemistry (Vol. 7, Issue 6, pp. 675–676). Future Science. https://doi.org/10.4155/fmc.15.27

35. Caffrey, C. R. (2007). Chemotherapy of schistosomiasis: present and future. In Current Opinion in Chemical Biology (Vol. 11, Issue 4, pp. 433–439). Curr Opin Chem Biol. https://doi.org/10.1016/j.cbpa.2007.05.031

36. Fallon, P. G. (1998). Schistosome resistance to praziquantel. In Drug Resistance Updates (Vol. 1, Issue 4, pp. 236–241). Churchill Livingstone. https://doi.org/10.1016/S1368-7646(98)80004-6

37. Vale, N., Gouveia, M. J., Rinaldi, G., Brindley, P. J., Gärtner, F., & Da Costa, J. M. C. (2017). Praziquantel for schistosomiasis: Single-drug metabolism revisited, mode of action, and resistance. In Antimicrobial Agents and Chemotherapy (Vol. 61, Issue 5). American Society for Microbiology. https://doi.org/10.1128/AAC.02582-16

38. Park, S. K., Gunaratne, G. S., Chulkov, E. G., Moehring, F., McCusker, P., Dosa, P. I., Chan, J. D., Stucky, C. L., & Marchant, J. S. (2019). The anthelmintic drug praziquantel activates a schistosome transient receptor potential channel. Journal of Biological Chemistry, 294(49), 18873–18880. https://doi.org/10.1074/jbc.AC119.011093

39. Xie, S. C., Dick, L. R., Gould, A., Brand, S., & Tilley, L. (2019). The proteasome as a target for protozoan parasites. Expert Opinion on Therapeutic Targets, 23(11), 903–914. https://doi.org/10.1080/14728222.2019.1685981

40. Abdulla, M. H., Lim, K. C., Sajid, M., McKerrow, J. H., & Caffrey, C. R. (2007). Schistosomiasis mansoni: Novel chemotherapy using a cysteine protease inhibitor. PLoS Medicine, 4(1), 0130–0138. https://doi.org/10.1371/journal.pmed.0040014

41. Abdulla, M. H., Ruelas, D. S., Wolff, B., Snedecor, J., Lim, K. C., Xu, F., Renslo, A. R., Williams, J., McKerrow, J. H., & Caffrey, C. R. (2009). Drug discovery for schistosomiasis: Hit and lead compounds identified in a library of known drugs by medium-throughput phenotypic screening. PLoS Neglected Tropical Diseases, 3(7). https://doi.org/10.1371/journal.pntd.0000478

42. Tanaka, K. (2009). The proteasome: Overview of structure and functions. In Proceedings of the Japan Academy Series B: Physical and Biological Sciences (Vol. 85, Issue 1, pp. 12–36). The Japan Academy. https://doi.org/10.2183/pjab.85.12

43. Caffrey, C. R., & Secor, W. E. (2011). Schistosomiasis: From drug deployment to drug development. In Current Opinion in Infectious Diseases (Vol. 24, Issue 5, pp. 410–417). Curr Opin Infect Dis. https://doi.org/10.1097/QCO.0b013e328349156f

44. Caffrey, C. R., El-Sakkary, N., Mäder, P., Krieg, R., Becker, K., Schlitzer, M., Drewry, D. H., Vennerstrom, J. L., & Grevelding, C. G. (2019). Drug Discovery and Development for Schistosomiasis. In Neglected Tropical Diseases: Drug Discovery and Development (pp. 187–225). wiley. https://doi.org/10.1002/9783527808656.ch8

45. Winzeler, E. A., & Ottilie, S. (2019). The proteasome as a target:How not tidying up can have toxic consequences for parasitic protozoa. In Proceedings of the National Academy of Sciences of the United States of America (Vol. 116, Issue 21, pp. 10198–10200). National Academy of Sciences. https://doi.org/10.1073/pnas.1904694116

46. Crunkhorn, S. (2016). Antiparasitic drugs: Proteasome inhibition combats kinetoplastid infections. In Nature Reviews Drug Discovery (Vol. 15, Issue 10, pp. 676–677). Nature Publishing Group. https://doi.org/10.1038/nrd.2016.190

47. Li, H., O'Donoghue, A. J., Van Der Linden, W. A., Xie, S. C., Yoo, E., Foe, I. T., Tilley, L., Craik, C. S., Da Fonseca, P. C. A., & Bogyo, M. (2016). Structure-and function-based design of Plasmodium-selective proteasome inhibitors. Nature, 530(7589), 233–236. https://doi.org/10.1038/nature16936

48. Wyllie, Susan, Stephen Brand, Michael Thomas, Manu De Rycker, Chun-wa Chung, Imanol Pena, Ryan P. Bingham, Juan A. Bueren-Calabuig, Juan Cantizani, David Cebrian, Peter D. Craggs, Liam Ferguson, Panchali Goswami, Judith Hobrath, Jonathan Howe, Laura Jeacock, Eun-Jung Ko, Justyna Korczynska, Lorna MacLean, Sujatha Manthri, Maria S. Martinez, Lydia Mata-Cantero, Sonia Moniz, Andrea Nühs, Maria Osuna-Cabello, Erika Pinto, Jennifer Riley, Sharon Robinson, Paul Rowland, Frederick R. Simeons, Yoko Shishikura, Daniel Spinks, Laste Stojanovski, John Thomas, Stephen Thompson, Elisabet Viayna Gaza, Richard J. Wall, Fabio Zuccotto, David Horn, Michael A. Ferguson, Alan H. Fairlamb, Jose M. Fiandor, Julio Martin, David W. Gray, Timothy J. Miles, Ian H. Gilbert, Kevin D. Read, Maria Marco, and Paul G. Wyatt. "Preclinical Candidate for the Treatment of Visceral Leishmaniasis That Acts through Proteasome Inhibition." *Proceedings of the National Academy of Sciences* 116.19 (2019): 9318-323. Print.

49. Bibo-Verdugo, B., Wang, S. C., Almaliti, J., Ta, A. P., Jiang, Z., Wong, D. A., Lietz, C. B., Suzuki, B. M., El-Sakkary, N., Hook, V., Salvesen, G. S., Gerwick, W. H., Caffrey, C. R., & O'Donoghue, A. J. (2019). The Proteasome as a Drug Target in the Metazoan Pathogen, Schistosoma mansoni. ACS Infectious Diseases, 5(10), 1802–1812. https://doi.org/10.1021/acsinfecdis.9b00237

50. Silva, L. L., Marcet-Houben, M., Nahum, L. A., Zerlotini, A., Gabaldón, T., & Oliveira, G. (2012). The Schistosoma mansoni phylome: Using evolutionary genomics to gain insight into a parasite's biology. BMC Genomics, 13(1), 617. https://doi.org/10.1186/1471-2164-13-617

51. Dimopoulos, M., Siegel, D., White, D. J., Boccia, R., Iskander, K. S., Yang, Z., Kimball, A. S., Mezzi, K., Ludwig, H., & Niesvizky, R. (2019). Carfilzomib vs bortezomib in patients with multiple myeloma and renal failure: A subgroup analysis of ENDEAVOR. Blood, 133(2), 147–155. https://doi.org/10.1182/blood-2018-06-860015

52. Shah, S. P., Nooka, A. K., Jaye, D. L., Bahlis, N. J., Lonial, S., & Boise, L. H. (2016). Bortezomib-induced heat shock response protects multiple myeloma cells and is activated by heat shock factor 1 serine 326 phosphorylation. Oncotarget, 7(37), 59727–59741. https://doi.org/10.18632/oncotarget.10847

53. Huang, H. H., Ferguson, I. D., Thornton, A. M., Bastola, P., Lam, C., Lin, Y. H. T., Choudhry, P., Mariano, M. C., Marcoulis, M. D., Teo, C. F., Malato, J., Phojanakong, P. J., Martin, T. G., Wolf, J. L., Wong, S. W., Shah, N., Hann, B., Brooks, A. N., & Wiita, A. P. (2020). Proteasome inhibitor-induced modulation reveals the spliceosome as a specific therapeutic vulnerability in multiple myeloma. Nature Communications, 11(1), 1–14. https://doi.org/10.1038/s41467-020-15521-4

54. Nagai, Yurie, Naoya Mimura, Ola Rizq, Yusuke Isshiki, Motohiko Oshima, Mohamed Rizk, Atsunori Saraya, Shuhei Koide, Yaeko Nakajima-Takagi, Makiko Miyota, Tetsuhiro Chiba, Nagisa Oshima-Hasegawa, Tomoya Muto, Shokichi Tsukamoto, Shio Mitsukawa, Yusuke Takeda, Chikako Ohwada, Masahiro Takeuchi, Tohru Iseki, Chiaki Nakaseko, William Lennox, Josephine Sheedy, Marla Weetall, Koutaro Yokote, Atsushi Iwama, and Emiko Sakaida. "The Combination of the Tubulin Binding Small Molecule PTC596 and Proteasome Inhibitors Suppresses the Growth of Myeloma Cells." *Scientific Reports* 11.1 (2021). Print.

55. Roeten, M. S. F., Cloos, J., & Jansen, G. (2018). Positioning of proteasome inhibitors in therapy of solid malignancies. In Cancer Chemotherapy and Pharmacology (Vol. 81, Issue 2, pp. 227–243). Springer Verlag. https://doi.org/10.1007/s00280-017-3489-0

56. Dou, Q., & Zonder, J. (2014). Overview of Proteasome Inhibitor-Based Anti-cancer Therapies: Perspective on Bortezomib and Second Generation Proteasome Inhibitors versus Future Generation Inhibitors of Ubiquitin-Proteasome System. Current Cancer Drug Targets, 14(6), 517–536. https://doi.org/10.2174/1568009614666140804154511

57. *Carfilzomib Versus Bortezomib: Comparing Proteasome Inhibitors in Newly Diagnosed Myeloma - ASH Clinical News*. (n.d.). Retrieved February 15, 2021, from https://www.ashclinicalnews.org/news/carfilzomib-versus-bortezomib-comparing-proteasome-inhibitors-newly-diagnosed-myeloma/

58. Bibo-Verdugo, B., Jiang, Z., Caffrey, C. R., & O'Donoghue, A. J. (2017). Targeting proteasomes in infectious organisms to combat disease. *The FEBS Journal*, *284*(10), 1503–1517. https://doi.org/10.1111/febs.14029

59. Verbist, B., Klambauer, G., Vervoort, L., Talloen, W., Shkedy, Z., Thas, O., Bender, A., Göhlmann, H. W. H., & Hochreiter, S. (2015). Using transcriptomics to guide lead optimization in drug discovery projects: Lessons learned from the QSTAR project. In Drug Discovery Today (Vol. 20, Issue 5, pp. 505–513). Elsevier Ltd. https://doi.org/10.1016/j.drudis.2014.12.014

60. Yang, X., Kui, L., Tang, M., Li, D., Wei, K., Chen, W., Miao, J., & Dong, Y. (2020). High-Throughput Transcriptome Profiling in Drug and Biomarker Discovery. In Frontiers in Genetics (Vol. 11, p. 19). Frontiers Media S.A. https://doi.org/10.3389/fgene.2020.00019

61. Duvall, R. H., & DeWitt, W. B. (1967). An improved perfusion technique for recovering adult schistosomes from laboratory animals. The American Journal of Tropical Medicine and Hygiene, 16(4), 483–486. https://doi.org/10.4269/ajtmh.1967.16.483

62. Colley, D. G., & Wikel, S. K. (1974). Schistosoma mansoni: Simplified method for the production of schistosomules. Experimental Parasitology, 35(1), 44–51. https://doi.org/10.1016/0014-4894(74)90005-8

63. Lu, Z., Sessler, F., Holroyd, N., Hahnel, S., Quack, T., Berriman, M., & Grevelding, C. G. (2017). Data Descriptor: A gene expression atlas of adult Schistosoma mansoni and their gonads. Scientific Data, 4(1), 1–9. https://doi.org/10.1038/sdata.2017.118

64. Love, M. I., Huber, W., & Anders, S. (2014). Moderated estimation of fold change and dispersion for RNA-seq data with DESeq2. Genome Biology, 15(12), 550. https://doi.org/10.1186/s13059-014-0550-8

65. ROSALIND. (n.d.). Retrieved January 21, 2021, from https://rosalind.onramp.bio

66. Luo, W. (2020). RNA-Seq Data Pathway and Gene-set Analysis Workflows. https://doi.org/10.1186/1471-2105-10-161

67. Brechtmann, F., Mertes, C., ci ut, M., Yépez, V. A., Avsec, Z., Herzog, M., Bader, D. M., Prokisch, H., & Gagneur, J. (2018). OUTRIDER: A Statistical Method for Detecting Aberrantly Expressed Genes in RNA Sequencing Data. https://doi.org/10.1016/j.ajhg.2018.10.025

68. Homer Software and Data Download. (n.d.). Retrieved February 4, 2021, from http://homer.ucsd.edu/homer/

69. Koetsier, G., Cantor, E., & Biolabs, E. (n.d.). A Practical Guide to Analyzing Nucleic Acid Concentration and Purity with Microvolume Spectrophotometers.

70. Primer designing tool. (n.d.). Retrieved February 4, 2021, from https://www.ncbi.nlm.nih.gov/tools/primer-blast/

71. Custom DNA Oligos | Thermo Fisher Scientific - US. (n.d.). Retrieved January 22, 2021, from https://www.thermofisher.com/us/en/home/life-science/oligonucleotides-primers-probes-genes/custom-dna-oligos.html

72. Sreedharan, S. P., Kumar, A., & Giridhar, P. (2018). Primer design and amplification efficiencies are crucial for reliability of quantitative PCR studies of caffeine biosynthetic N-methyltransferases in coffee. 3 Biotech, 8(11), 467. https://doi.org/10.1007/s13205-018-1487-5

73. qPCR Efficiency Calculator | Thermo Fisher Scientific - US. (n.d.). Retrieved January 22, 2021, from https://www.thermofisher.com/us/en/home/brands/thermo-scientific/molecular-biology/molecular-biology-learning-center/molecular-biology-resource-library/thermo-scientific-web-tools/qpcr-efficiency-calculator.html

74. Understanding qPCR Efficiency and Why It Exceeds 100% | BioSistemika. (n.d.). Retrieved February 13, 2021, from https://biosistemika.com/blog/qpcr-efficiency-over-100/

75. Zhang, A. N., Mao, Y., & Zhang, T. (2016). Development of Quantitative Real-time PCR Assays for Different Clades of "Candidatus Accumulibacter." Scientific Reports, 6. https://doi.org/10.1038/srep23993

76. Svec, D., Tichopad, A., Novosadova, V., Pfaffl, M. W., & Kubista, M. (2015). How good is a PCR efficiency estimate: Recommendations for precise and robust qPCR efficiency assessments. Biomolecular Detection and Quantification, 3, 9–16. https://doi.org/10.1016/j.bdq.2015.01.005

77. Livak, K. J., & Schmittgen, T. D. (2001). Analysis of relative gene expression data using real-time quantitative PCR and the 2-ΔΔCT method. Methods, 25(4), 402–408. https://doi.org/10.1006/meth.2001.1262

78. Nucleotide BLAST: Search nucleotide databases using a nucleotide query. (n.d.). Retrieved February 4, 2021, from https://blast.ncbi.nlm.nih.gov/Blast.cgi?LINK_LOC=blasthome&PAGE_TYPE=BlastSearch&PROGRAM=blastn

79. Protein BLAST: search protein databases using a protein query. (n.d.). Retrieved January 22, 2021, from https://blast.ncbi.nlm.nih.gov/Blast.cgi?PAGE=Proteins

80. KEGG: Kyoto Encyclopedia of Genes and Genomes. (n.d.). Retrieved February 4, 2021, from https://www.kegg.jp/

81. Takayama, S., Xie, Z., & Reed, J. C. (1999). An evolutionarily conserved family of Hsp70/Hsc70 molecular chaperone regulators. Journal of Biological Chemistry, 274(2), 781–786. https://doi.org/10.1074/jbc.274.2.781

82. Yu, J., Cheng, Y., Feng, K., Ruan, M., Ye, Q., Wang, R., Li, Z., Zhou, G., Yao, Z., Yang, Y., & Wan, H. (2016). Genome-Wide Identification and Expression Profiling of Tomato

Hsp20 Gene Family in Response to Biotic and Abiotic Stresses. Frontiers in Plant Science, 7(AUG2016), 1215. https://doi.org/10.3389/fpls.2016.01215

83. Ran, R., Lu, A., Xu, H., Tang, Y., & Sharp, F. R. (2007). Heat-shock protein regulation of protein folding, protein degradation, protein function, and apoptosis. In Handbook of Neurochemistry and Molecular Neurobiology: Acute Ischemic Injury and Repair in the Nervous System (pp. 89–107). Springer US. https://doi.org/10.1007/978-0-387-30383-3_6

84. Awasthi, N., & Wagner, B. J. (2005). Upregulation of heat shock protein expression by proteasome inhibition: An antiapoptotic mechanism in the lens. Investigative Ophthalmology and Visual Science, 46(6), 2082–2091. https://doi.org/10.1167/iovs.05-0002

85. Zügel, U., & Kaufmann, S. H. E. (1999). Role of heat shock proteins in protection from and pathogenesis of infectious diseases. In Clinical Microbiology Reviews (Vol. 12, Issue 1, pp. 19–39). American Society for Microbiology. https://doi.org/10.1128/cmr.12.1.19

86. Ritossa, F. (1962). A new puffing pattern induced by temperature shock and DNP in drosophila. Experientia, 18(12), 571–573. https://doi.org/10.1007/BF02172188

87. Asea, A. (2005). Stress proteins and initiation of immune response: Chaperokine activity of Hsp72. In Exercise Immunology Review (Vol. 11, pp. 34–45). NIH Public Access. /pmc/articles/PMC1762141/

88. HSP-Molecular Chaperones in Cancer Biogenesis and Tumor Therapy: An Overview | Anticancer Research. (n.d.). Retrieved March 31, 2021, from https://ar.iiarjournals.org/content/32/12/5139

89. Sayeed, S. K., Shah, V., Chaubey, S., Singh, M., Alampalli, S. V., & Tatu, U. S. (2014). Identification of heat shock factor binding protein in Plasmodium falciparum. Malaria Journal, 13(1), 118. https://doi.org/10.1186/1475-2875-13-118

90. Day, J., Passecker, A., Beck, H. P., & Vakonakis, I. (2019). The Plasmodium falciparum Hsp70-x chaperone assists the heat stress response of the malaria parasite. FASEB Journal : Official Publication of the Federation of American Societies for Experimental Biology, 33(12), 14611–14624. https://doi.org/10.1096/fj.201901741R

91. Hedstrom, R., Culpepper, J., Harrison, R. A., Agabian, N., & Newport, G. (n.d.). *A MAJOR IMMUNOGEN IN SCHISTOSOMA MANSONI INFECTIONS IS HOMOLOGOUS TO THE HEAT-SHOCK PROTEIN Hsp70*.

92. Kanamura, H. Y., Hancock, K., Rodrigues, V., & Damian, R. T. (2002). Schistosoma mansoni heat shock protein 70 elicits an early humoral immune response in *S. mansoni* infected baboons. Memorias Do Instituto Oswaldo Cruz, 97(5), 711–716. https://doi.org/10.1590/S0074-02762002000500022

93. Ishida, K., & Jolly, E. R. (2016). Hsp70 May Be a Molecular Regulator of Schistosome Host Invasion. PLOS Neglected Tropical Diseases, 10(9), e0004986. https://doi.org/10.1371/journal.pntd.0004986

94. Horwitz, J. (1992). α-Crystallin can function as a molecular chaperone. Proceedings of the National Academy of Sciences of the United States of America, 89(21), 10449–10453. https://doi.org/10.1073/pnas.89.21.10449

95. Silver, J. T., & Noble, E. G. (2012). Regulation of survival gene hsp70. In Cell Stress and Chaperones (Vol. 17, Issue 1, pp. 1–9). Springer. https://doi.org/10.1007/s12192-011-0290-6

96. Fan, G. C., Ren, X., Qian, J., Yuan, Q., Nicolaou, P., Wang, Y., Jones, W. K., Chu, G., & Kranias, E. G. (2005). Novel cardioprotective role of a small heat-shock protein, Hsp20, against ischemia/reperfusion injury. Circulation, 111(14), 1792–1799. https://doi.org/10.1161/01.CIR.0000160851.41872.C6

97. Verschuure, P., Croes, Y., Van Den IJssel, P. R. L. A., Quinlan, R. A., De Jong, W. W., & Boelens, W. C. (2002). Translocation of small heat shock proteins to the actin cytoskeleton upon proteasomal inhibition. Journal of Molecular and Cellular Cardiology, 34(2), 117–128. https://doi.org/10.1006/jmcc.2001.1493

98. Cao, M., Chao, H., & Doughty, B. L. (1993). Cloning of a cDNA encoding an egg antigen homologue from Schistosoma mansoni. Molecular and Biochemical Parasitology, 58(1), 169–171. https://doi.org/10.1016/0166-6851(93)90102-4

99. Knudsen, G. M., Medzihradszky, K. F., Lim, K. C., Hansell, E., & McKerrow, J. H. (2005). Proteomic analysis of Schistosoma mansoni cercarial secretions. Molecular and Cellular Proteomics, 4(12), 1862–1875. https://doi.org/10.1074/mcp.M500097-MCP200

100. Yew, E. H. J., Cheung, N. S., Choy, M. S., Qi, R. Z., Lee, A. Y.-W., Peng, Z. F., Melendez, A. J., Manikandan, J., Koay, E. S.-C., Chiu, L.-L., Ng, W. L., Whiteman, M., Kandiah, J., & Halliwell, B. (2005). Proteasome inhibition by lactacystin in primary neuronal cells induces both potentially neuroprotective and pro-apoptotic transcriptional responses: a microarray analysis. Journal of Neurochemistry, 94(4), 943–956. https://doi.org/10.1111/j.1471-4159.2005.03220.x

101. Eugênio, A. I. P., Fook-Alves, V. L., de Oliveira, M. B., Fernando, R. C., Zanatta, D. B., Strauss, B. E., Silva, M. R. R., Porcionatto, M. A., & Colleoni, G. W. B. (2017). Proteasome and heat shock protein 70 (HSP70) inhibitors as therapeutic alternative in multiple myeloma. Oncotarget, 8(70), 114698–114709. https://doi.org/10.18632/oncotarget.22815

102. Young, J. T. F., & Heikkila, J. J. (2010). Proteasome inhibition induces hsp30 and hsp70 gene expression as well as the acquisition of thermotolerance in Xenopus laevis A6 cells. Cell Stress and Chaperones, 15(3), 323–334. https://doi.org/10.1007/s12192-009-0147-4

103. Albornoz, N., Bustamante, H., Soza, A., & Burgos, P. (2019). Molecular Sciences Cellular Responses to Proteasome Inhibition: Molecular Mechanisms and Beyond. https://doi.org/10.3390/ijms20143379

104. Lundgren, J., Masson, P., Mirzaei, Z., & Young, P. (2005). Identification and Characterization of a Drosophila Proteasome Regulatory Network. Molecular and Cellular Biology, 25(11), 4662–4675. https://doi.org/10.1128/mcb.25.11.4662-4675.2005

105. Ring, C., Ginsberg, M. H., Haling, J., & Pendergast, A. M. (2011). Abl-interactor-1 (Abi1) has a role in cardiovascular and placental development and is a binding partner of the α4 integrin. Proceedings of the National Academy of Sciences of the United States of America, 108(1), 149–154.https://doi.org/10.1073/pnas.1012316108

106. Zieger, H. L., Kunde, S. A., Rademacher, N., Schmerl, B., & Shoichet, S. A. (2020). Disease-associated synaptic scaffold protein CNK2 modulates PSD size and influences localisation of the regulatory kinase TNIK. Scientific Reports, 10(1), 1–14. https://doi.org/10.1038/s41598-020-62207-4

107. Heberle, A. M., Rehbein, U., Peiris, M. R., & Thedieck, K. (2021). Finding new edges: Systems approaches to MTOR signaling. In Biochemical Society Transactions (Vol. 49, Issue 1, pp. 41–54). Portland Press Ltd. https://doi.org/10.1042/BST20190730

108. Efeyan, A., & Sabatini, D. M. (2010). MTOR and cancer: Many loops in one pathway. In Current Opinion in Cell Biology (Vol. 22, Issue 2, pp. 169–176). NIH Public Access. https://doi.org/10.1016/j.ceb.2009.10.007

109. Kaizuka, T., Hara, T., Oshiro, N., Kikkawa, U., Yonezawa, K., Takehana, K., Iemura, S. I., Natsume, T., & Mizushima, N. (2010). Tti1 and Tel2 are critical factors in mammalian target of rapamycin complex assembly. Journal of Biological Chemistry, 285(26), 20109–20116. https://doi.org/10.1074/jbc.M110.121699

110. Lazo, J. S., McQueeney, K. E., & Sharlow, E. R. (2017). New Approaches to Difficult Drug Targets: The Phosphatase Story. In SLAS Discovery (Vol. 22, Issue 9, pp. 1071–1083). SAGE Publications Inc. https://doi.org/10.1177/2472555217721142

111. Moreno-Cinos, C., Goossens, K., Salado, I. G., Van Der Veken, P., De Winter, H., & Augustyns, K. (2019). ClpP protease, a promising antimicrobial target. In International Journal of Molecular Sciences (Vol. 20, Issue 9). MDPI AG. https://doi.org/10.3390/ijms20092232

112. Ali, M. S., & Baek, K. H. (2020). Protective roles of cytosolic and plastidal proteasomes on abiotic stress and pathogen invasion. Plants, 9(7), 1–17. https://doi.org/10.3390/plants9070832

113. Sun, Y., Thompson, M., Lin, G., Butler, H., Gao, Z., Thornburgh, S., Yau, K., Smith, D. A., & Shukla, V. K. (2007). Inositol 1,3,4,5,6-pentakisphosphate 2-kinase from maize: Molecular and biochemical characterization. Plant Physiology, 144(3), 1278–1291. https://doi.org/10.1104/pp.107.095455

114. Bohn, L., Meyer, A. S., & Rasmussen, S. K. (2008). Phytate: Impact on environment and human nutrition. A challenge for molecular breeding. In Journal of Zhejiang University: Science B (Vol. 9, Issue 3, pp. 165–191). Zhejiang University Press. https://doi.org/10.1631/jzus.B0710640

115. Verbsky, J., Lavine, K., & Majerus, P. W. (2005). Disruption of the mouse inositol 1,3,4,5,6-pentakisphosphate 2-kinase gene, associated lethality, and tissue distribution of 2-kinase expression. Proceedings of the National Academy of Sciences of the United States of America, 102(24), 8448–8453. https://doi.org/10.1073/pnas.0503656102

116. Paul, M. K., & Mukhopadhyay, A. K. (2012). Tyrosine kinase – Role and significance in Cancer. International Journal of Medical Sciences, 1(2), 101–115. https://doi.org/10.7150/ijms.1.101

117. Crawford, L. J., Chan, E. T., Aujay, M., Holyoake, T. L., Melo, J. V., Jorgensen, H. G., Suresh, S., Walker, B., & Irvine, A. E. (2014). Synergistic effects of proteasome inhibitor carfilzomib in combination with tyrosine kinase inhibitors in imatinib-sensitive and-resistant chronic myeloid leukemia models. Oncogenesis, 3(3), e90–e90. https://doi.org/10.1038/oncsis.2014.3

118. Wang, Z., Gerstein, M., & Snyder, M. (2009). RNA-Seq: A revolutionary tool for transcriptomics. In Nature Reviews Genetics (Vol. 10, Issue 1, pp. 57–63). NIH Public Access. https://doi.org/10.1038/nrg2484

119. Stark, R., Grzelak, M., & Hadfield, J. (2019). RNA sequencing: the teenage years. In Nature Reviews Genetics (Vol. 20, Issue 11, pp. 631–656). Nature Publishing Group. https://doi.org/10.1038/s41576-019-0150-2

120. Gray, J. M., Harmin, D. A., Boswell, S. A., Cloonan, N., Mullen, T. E., Ling, J. J., Miller, N., Kuersten, S., Ma, Y.-C., McCarroll, S. A., Grimmond, S. M., & Springer, M. (2014). SnapShot-Seq: A Method for Extracting Genome-Wide, In Vivo mRNA Dynamics from a Single Total RNA Sample. PLoS ONE, 9(2), e89673. https://doi.org/10.1371/journal.pone.0089673

121. Rajkumar, A. P., Qvist, P., Lazarus, R., Lescai, F., Ju, J., Nyegaard, M., Mors, O., Børglum, A. D., Li, Q., & Christensen, J. H. (2015). Experimental validation of methods for differential gene expression analysis and sample pooling in RNA-seq. BMC Genomics, 16(1), 548. https://doi.org/10.1186/s12864-015-1767-y

122. Rizq, O., Mimura, N., Oshima, M., Saraya, A., Koide, S., Kato, Y., Aoyama, K., Nakajima-Takagi, Y., Wang, C., Ma, A., Jin, J., Iseki, T., Nakaseko, C., & Iwama, A. (2016). Molecular Mechanism behind the Synergistic Activity of Proteasome Inhibition and PRC2 Inhibition in the Treatment of Multiple Myeloma. Blood, 128(22), 312–312. https://doi.org/10.1182/blood.v128.22.312.312